ASSESSMENT OF A POTENTIAL THERAPEUTIC TARGET IN THE HEDGEHOG PATHWAY FOR THE ERADICATION OF PRIMITIVE CHRONIC MYELOID LEUKEMIA CELLS

by

Kelly Anne Turner

B.Sc., The University of Victoria, 2015

A THESIS SUBMITTED IN PARTIAL FULFILLMENT OF

THE REQUIREMENTS FOR THE DEGREE OF

MASTER OF SCIENCE

in

THE FACULTY OF GRADUATE AND POSTDOCTORAL STUDIES

(Medical Genetics)

THE UNIVERSITY OF BRITISH COLUMBIA

(Vancouver)

August 2017

ABSTRACT

Chronic myeloid leukemia (CML) is a hematological malignancy characterized by the presence of a novel fusion oncoprotein called BCR-ABL1 in a hematopoietic stem cell. BCR-ABL1 has constitutively active tyrosine kinase activity and deregulates many intracellular signaling pathways contributing to cancer formation, maintenance, and progression.

The consistent genetic aberration of BCR-ABL1 in CML led to the development of the first molecularly-targeted cancer therapy called imatinib (IM), which revolutionized the treatment of early phase CML. However, IM is not curative, and 40% of patients with advanced CML experience primary intolerance or acquire resistance to IM. In addition, leukemic stem cells (LSCs) are relatively insensitive to IM and do not exclusively rely on BCR-ABL1 for survival. Therefore, it is important to investigate alternative pathways that are critical for LSC maintenance, to develop a strategy to eradicate them.

The Hedgehog (HH) pathway, and particularly the protein Smoothened (SMO), has recently been described to be essential for CML LSCs in a mouse model. I hypothesized that the HH pathway was critical for the survival of CML stem/progenitor cells, and that dual inhibition of BCR-ABL1 and SMO would be superior to either alone in killing CML LSCs. I used a variety of biological and molecular assays to investigate expression changes of several HH pathway-associated genes and the functionality of different leukemic cell subsets from primary CML patient samples.

I observed that HH pathway genes *SMO* and *GLI2* were upregulated in CML compared with healthy bone marrow controls, and were more highly expressed in CD34$^+$ cells from IM non-responders as compared with responders. In addition, these genes were most highly

expressed in the stem cell-enriched $Lin^-CD34^+CD38^-$ subpopulation in IM non-responders compared with progenitors and mature leukemic cells in the same patients. I also observed that $CD34^+$ IM non-responder cells were more sensitive to SMO inhibition compared with responders in terms of viability, apoptosis, re-plating potential, and colony-forming ability following long-term culture.

Taken together, my results support the hypothesis that the HH pathway is more critical for primitive CML cells from IM non-responders, and may represent a mechanism by which drug-resistant cells evade eradication by TKIs.

LAY SUMMARY

Chronic myeloid leukemia (CML) is a blood cancer with an effective treatment strategy for some patients. However, in others, the treatment fails due to the persistence of drug-resistant cells in their blood and bone marrow. In order to evade eradication, these cells will use other cellular pathways that promote their survival. One such pathway is the Hedgehog (HH) pathway. In my study, I observed that expression of HH pathway genes was elevated in CML cells, and to the greatest extent in the most primitive CML cells, particularly from patients that did not respond to the standard treatment. I also observed that more of these cells could be eliminated when given a combination of the standard treatment with a HH pathway inhibitor. My results suggest that this combination therapy may represent a treatment option for CML patients that do not respond well to conventional therapies.

PREFACE

Under the supervision of Dr. Xiaoyan Jiang and in collaboration with Dr. Adrian Woolfson at Pfizer, Inc., I designed the experiments described in this thesis with assistance from Dr. Katharina Rothe. I performed all of the biological assays related to this work, RNA sequencing and analysis was performed by my colleague Dr. Hanyang Lin, with assistance from Dr. Ryan Brinkman's group, and some qRT-PCR data was supplied by Dr. Rothe.

TABLE OF CONTENTS

LIST OF TABLES

LIST OF FIGURES

LIST OF ABBREVIATIONS

AML	acute myeloid leukemia
AMN	nilotinib
AP-CML	accelerated phase chronic myeloid leukemia
APC	allophycocyanin
BC-CML	blast crisis chronic myeloid leukemia
BCR-ABL1	breakpoint cluster region-Abelson murine leukemia viral oncogene homolog 1
BOS	bosutinib
CCyR	complete cytogenetic response
CFC	colony-forming cell
CFU	colony-forming unit
CLP	common lymphoid progenitor
CML	chronic myeloid leukemia
CMP	common myeloid progenitor
CP-CML	chronic phase chronic myeloid leukemia
DA	dasatinib
ES	embryonic stem
GEM	granulocyte/erythroid/macrophage
GMP	granulocyte-macrophage progenitor
HBM	healthy bone marrow
HBSS	Hank's Balanced Salt Solution

HH	Hedgehog
HSC	hematopoietic stem cell
IC_{50}	inhibitory concentration 50%
IM	imatinib mesylate
iPS	induced pluripotent stem
LSC	leukemic stem cell
LTC-IC	long-term culture-initiating cell
LT-HSC	long-term hematopoietic stem cell
MDM	Modified Dulbecco's Medium
MDS	myelodysplastic syndrome
MEP	megakaryocyte-erythroid progenitor
MMR	major molecular response
mOS	median overall survival
MPP	multi-potent progenitor
NPC	neural progenitor cell
PB	peripheral blood
PCyR	partial cytogenetic response
PF913	PF-04449913, SMO inhibitor
Ph	Philadelphia chromosome
PI	propidium iodide
qRT-PCR	quantitative real time polymerase chain reaction
rIFN-α	recombinant interferon alpha

RNA-seq	RNA sequencing
RPKM	reads per kilobase of transcript per million mapped reads
SCT	stem cell transplantation
SMO	Smoothened
ST-HSC	short-term hematopoietic stem cell
TKI	tyrosine kinase inhibitor

ACKNOWLEDGEMENTS

This thesis is dedicated to all of my scientific mentors,

past and present,

who kept me engaged, passionate, and curious

CHAPTER 1 INTRODUCTION

1.1   CML

1.1.1   Background

Chronic myeloid leukemia (CML) is a potentially lethal hematologic malignancy characterized by a reciprocal chromosomal translocation between the long arms of chromosomes 9 and 22 t(9;22) in a hematopoietic stem cell (HSC). First described by Nowell and Hungerford in 1960 (Nowell & Hungerford, 1960), the "minute" chromosome was later referred to as the Philadelphia chromosome (Ph) by Tough and colleagues from the University of Pennsylvania (Tough *et al.,* 1961). It was not until more than a decade later, when chromosomal banding techniques had improved, that Janet Rowley determined that this small chromosome was indeed the result of a chromosomal translocation (Rowley, 1972). While the precise chromosomal location of the breakpoints varies, all translocations result in the juxtaposition of the breakpoint cluster region (*BCR*) gene on chromosome 22 and the Abelson murine leukemia viral oncogene homolog 1 (*ABL1*) on chromosome 9, resulting in the formation of an oncogenic fusion gene, *BCR-ABL1*. The loss of regulatory elements upstream of *ABL1* upon fusion with *BCR* render the tyrosine kinase domain of ABL1 constitutively active, promoting autophosphorylation and activation of many intracellular signaling proteins involved in proliferation (Massimino *et al.,* 2014), evasion of apoptosis (Jagani *et al.,* 2008), autophagy (Rothe *et al.,* 2014), cell cycle (Gesbert *et al.,* 2000), and genome stability (Koptyra *et al.,* 2006), among others (Figure 1.1). The deregulation of these pathways, including RAS/MAPK, JAK/STAT, and PI3K/AKT, drive the malignancy (Steelman *et al.,* 2004).
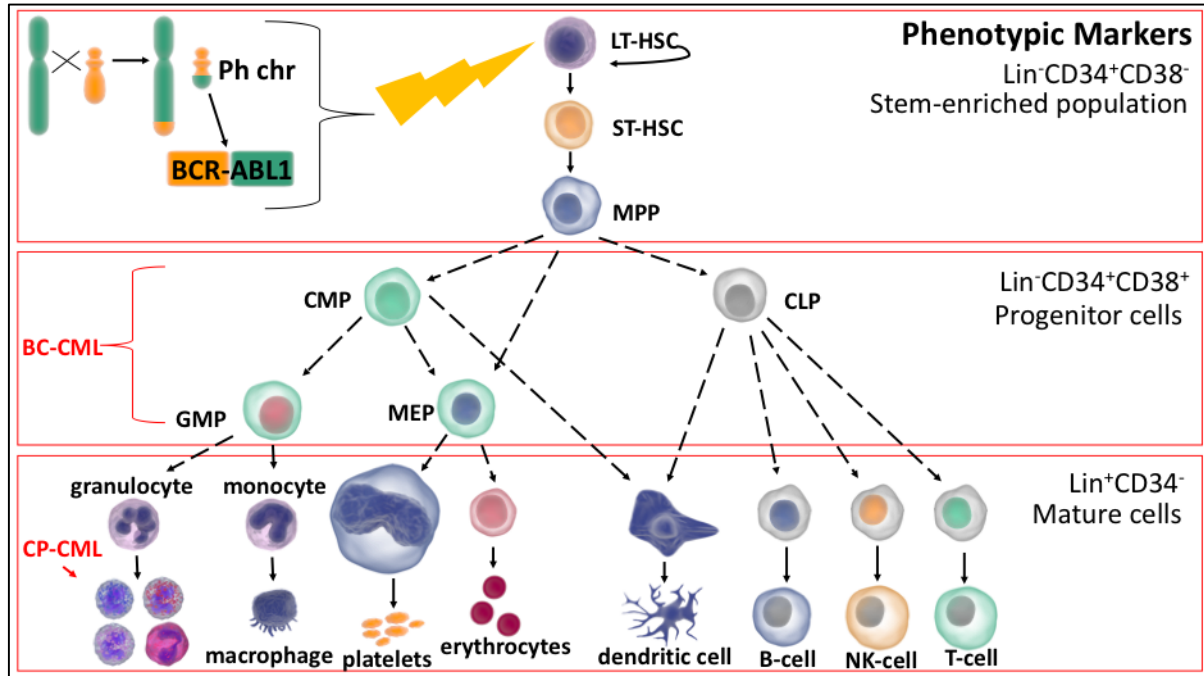
Figure 1.1 **Overview of the classical hematopoietic hierarchy and CML.** Schematic detailing the cell of origin in CML, the long-term hematopoietic stem cell (LT-HSC). This cell is able to give rise to all hematopoietic cell types by the successive constriction of differentiation potential, while also retaining the capacity for self-renewal. Chronic phase CML (CP-CML) is characterized by an increased number of mature granulocytes in the peripheral blood (PB) and bone marrow (BM), whereas the terminal phase of the disease, blast crisis (BC) CML is characterized by an increased number of cells with features of myeloid or lymphoid progenitors that are blocked in their ability to differentiate further. The red boxes delineate the shared characteristics of groups of hematopoietic cells according to their differentiation potential and can be separated according to the presence or absence of particular cell surface markers. ST-HSC = short-term hematopoietic stem cell. MPP = multi-potent progenitor. CMP = common myeloid progenitor. CLP = common lymphoid progenitor. GMP = granulocyte-macrophage progenitor. MEP = megakaryocyte-erythroid progenitor. Figure adapted from Weissman & Shizuru, 2008.

CML occurs at a frequency of approximately 1 in 100,000 people in the general population and represents approximately 12% of new leukemia diagnoses. CML has a slight male bias, and the median age at diagnosis is 64 years (Canadian Cancer Statistics, 2016). Initial symptoms of the disease may include fatigue, general malaise, weight loss, and discomfort caused by splenomegaly (Quintas-Cardama & Cortes, 2006). Due to the mild

nature of these symptoms, CML is commonly detected as a secondary finding in routine blood work, first recognized as an increased white blood cell count. If inadequately treated, the disease follows a triphasic course, beginning with the chronic phase. Chronic phase CML (CP-CML) is characterized by an increased number of granulocytes in the peripheral blood (PB) and bone marrow (BM) and accompanied by other hematologic findings such as mild to moderate anemia, and an increase in basophils and eosinophils (Quintas-Cardama & Cortes, 2006). A diagnostic criterion of CML is the detection of the Ph chromosome by karyotype or fluorescence in-situ hybridization (FISH) and/or the detection of *BCR-ABL1* transcripts by reverse transcription PCR (RT-PCR). If no treatment is initiated or it is inadequate, the disease will progress to the accelerated phase (AP-CML), which is characterized by the detection 15-29% immature myeloid cells in PB and BM and then usually rapidly to a terminal stage referred to as the blast phase or blast crisis (BC-CML) that closely resembles an aggressive acute leukemia. BC-CML is characterized by >30% immature myeloid blasts in the PB and BM (Baccarani *et al.,* 2013). At this stage, the disease is usually relatively refractory to any current treatment, due to the numerous new mutations acquired by cells in the leukemic clone (Grossman *et al.,* 2011; Kim *et al.,* 2017), and death typically ensues within months.

1.1.2   CML Treatment

As early as the 19th century, what was thought to be CML was described in the literature (Bennet, 1845). Treatments initially included arsenic-containing compounds (Conan-Doyle, 1882) and later radiotherapy and alkylating agents such as busulfan (Haut *et al.,* 1961) and hydroxyurea (Kennedy & Yarbro, 1966). While busulfan and hydroxyurea could normalize blood counts and alleviate symptoms, they were unable to prevent disease

progression and median survival was approximately 2.7 and 5.6 years, respectively (Hehlmann *et al.,* 1993). Disease progression was due to the persistence of Ph$^+$ cells, and so therapies that could target these cells were clearly needed. In the 1970's, allogeneic stem cell transplantation (SCT) was first described (Fefer *et al.,* 1979) and associated with prolonged survival (McGlave *et al*., 1994), with complete and permanent cytogenetic remissions possible for some patients. SCT remains the only curative therapy for CML; however, it is associated with significant morbidity and mortality due to infections and graft-versus-host disease (Speck *et al.,* 1984) and it is only available to patients with a suitable donor. Another treatment strategy was recombinant human interferon (rIFN-α). rIFN-α increased median survival and demonstrated a cytogenetic response compared to chemotherapy (Hehlmann *et al.,* 1994), but was associated with considerable adverse events including muscle pain, nausea, vomiting, hair loss, and depression, among others (Talpaz *et al.,* 1986).

CML therapy was revolutionized when Levitzki and colleagues hypothesized that it might be possible to treat ABL-associated human leukemias with specific ABL kinase inhibitors (Anafi *et al.,* 1992). In 1996, Druker et al. demonstrated that a compound called CGP57148, later STI571, and now referred to as imatinib mesylate (IM), could inhibit cellular proliferation, colony formation, and regeneration of disease in mice transplanted with BCR-ABL1-expressing cells (Druker *et al.,* 1996). Mechanistically, IM selectively inhibits the ABL1 protein kinase by blocking the binding of adenosine triphosphate, preventing the phosphorylation of downstream targets that drive the production of the leukemia cells. In the phase I clinical trial in CP-CML patients with previous rIFN-α treatment failure, 98% achieved a complete hematological response with daily doses of >300 mg IM. In addition, 54% of

4

patients treated with >300 mg daily had major or minor cytogenetic responses, with 13% achieving complete cytogenetic remission in a relatively short time frame (Druker *et al.,* 2001). Shortly after, the IRIS study (international randomized study of interferon and cytarabine versus STI571), which included 1100 newly-diagnosed CML patients, published results that revolutionized the treatment and management of CML. In particular, at a median follow-up of 18 months, 76% of the patients in the IM arm achieved complete cytogenetic remission, and 40% achieved a 3-log reduction in BCR-ABL1 transcripts by 12 months (O'Brien *et al.,* 2003). After 8 years of follow-up, event-free survival for patients on IM was 81%, and progression-free survival was 92% (Deininger *et al.,* 2009).

1.1.3   IM Treatment Challenges

Unfortunately, IM is not curative and not all patients respond to the drug, particularly if treatment is initiated at in AP (Talpaz *et al.,* 2002) or BC (Sawyers *et al.,* 2002). The absence of efficacy (primary resistance), loss of a previously-attained response (acquired resistance), and/or intolerance to therapy also remain significant issues. BCR-ABL1-dependent factors that may contribute to primary or acquired resistance include *BCR-ABL1* gene amplification (le Coutre *et al.,* 2000) and the development of point mutations in the ABL1 kinase domain, which decrease drug binding (Gorre *et al.,* 2001). BCR-ABL1-independent mechanisms of resistance include decreased influx or increased efflux of IM through deregulation of drug transporter proteins (Illmer *et al.,* 2004; Jiang *et al.,* 2007; Wang *et al.,* 2008), contact with BM mesenchymal stromal cells (Vianello *et al.,* 2010), and the activation of other pro-survival pathways including autophagy (Rothe *et al.,* 2014) and possibly the Hedgehog (HH) pathway (Dierks *et al.,* 2008; Zhao *et al.,* 2009) (Figure 1.2), among others (Burchert *et al.,* 2005; Wang

et al., 2007; Agarwal *et al.,* 2008; Gioia *et al.,* 2011). In addition, primitive, quiescent leukemic stem cells (LSCs) do not rely on BCR-ABL1 activity for their survival, and are often responsible for disease relapse once therapy with tyrosine kinase inhibitors (TKIs) has been discontinued (Holyoake *et al.,* 1999; Jiang *et al.,* 2007; Mahon *et al.,* 2010; Corbin *et al.,* 2011; Hamilton *et al.,* 2012) (Figure 1.2).
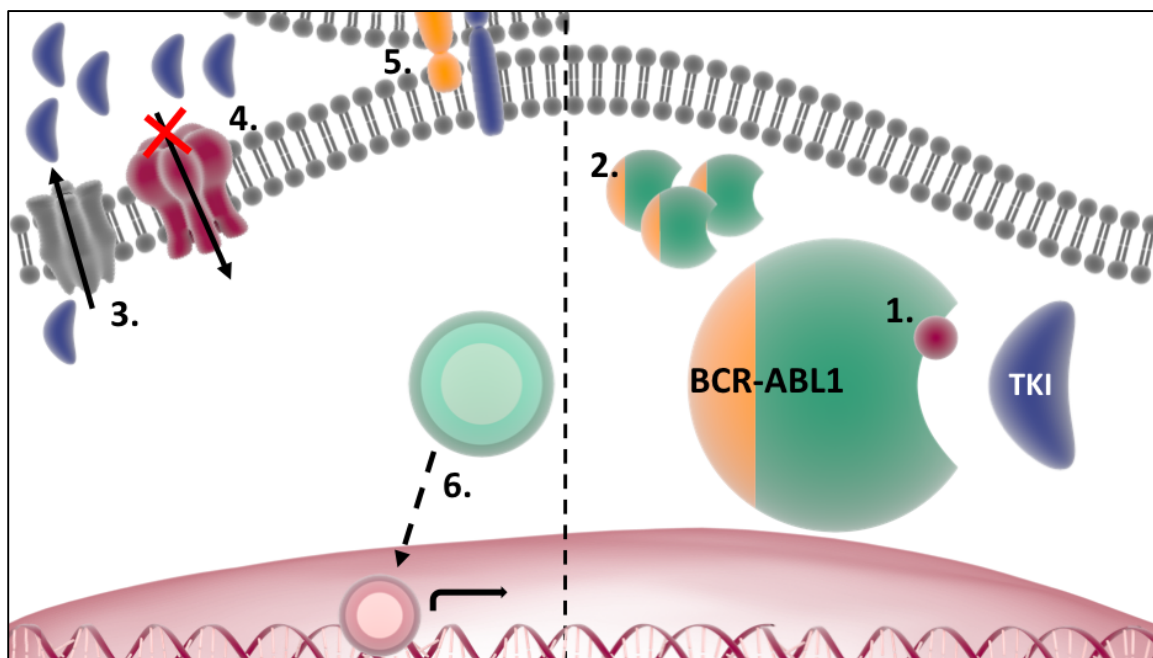
Figure 1.2   Mechanisms of TKI resistance in CML. The right side of the figure outlines BCR-ABL1-dependent mechanisms of resistance including 1. BCR-ABL1 kinase domain mutations and 2. Increases in BCR-ABL1 expression or amplification of the BCR-ABL1 gene. The left side of the figure outlines BCR-ABL1-independent mechanisms of TKI resistance including 3. Increased TKI efflux and 4. Decreased TKI influx. Other mechanisms include 5. Contact with the protective BM stromal cells and 6. The activation of other pro-survival pathways, including the Hedgehog (HH) pathway.

1.1.4   2nd Generation TKIs Including Bosutinib (BOS)

To combat the issue of kinase-specific mutations promoting resistance to IM, as well as other resistance/intolerance mechanisms, second and more recently, third generation ABL1

TKIs have been developed. They include dasatinib (DA), nilotinib (AMN), BOS; and ponatinib. IM remains the standard first-line therapy for many CML patients at diagnosis; however, DA and AMN have also been approved for first-line use in the U.S. and Europe. BOS in currently indicated for adult Ph^+ CML with resistance or intolerance to prior therapy (Wei *et al.,* 2010). For the purposes of this work, I will further emphasize what has been described about BOS exclusively, as it was the TKI utilized for my project.

BOS is an orally bioavailable dual SRC/ABL kinase inhibitor. Unlike the aforementioned TKIs, BOS does not inhibit other kinases such as the platelet-derived growth factor receptor and c-KIT (Boschelli *et al.,* 2001), which are associated with toxicities such as myelosuppression and pleural effusion in some patients (Giles *et al.,* 2009). In preclinical models, BOS potently inhibits cell proliferation and survival in CML cell lines with IC_{50}s ranging from 88 nM to 210 nM. Oral treatment of nude mice with K562 xenografts led to complete tumour regression for up to 64 days (Golas *et al.,* 2003). Importantly, BOS is also active against a number of IM-resistant BCR-ABL mutants including Q252H and L384M (insensitive to both DA and AMN). However, similar to DA and AMN, BOS cannot inhibit the "gatekeeper" mutation T315I (Redaelli *et al.,* 2009), which is insensitive to all TKIs except ponatinib (Cortes *et al.,* 2011a).

In a phase 1/2 clinical trial of BOS for IM-intolerant or IM-resistant CML patients, 31% of patients achieved a major cytogenetic response after 6 months. In addition, after a median follow-up of approximately 2 years, 86% of patients achieved complete hematologic remission. 53% of these achieved a major cytogenetic response. Progression-free survival was

79% and overall survival was 92% (Cortes *et al.,* 2011b). The results of this trial suggested that BOS was effective for IM-resistant or intolerant CML patients.

1.1.5   Disease Monitoring

With survival now measured in years for most CML patients on TKIs, guidelines have been put in place and continually updated for the management of what was once thought of as a lethal disease (Baccarani *et al.,* 2013). As stated previously, IM, DA, and AMN are all approved first-line therapies. Once TKI therapy has been initiated, response is measured by quantifying the amount of BCR-ABL1 transcripts relative to pre-treatment levels by qRT-PCR at 3, 6, and 12 months. In addition, detection of the Ph chromosome by FISH or karyotype at these time points is often employed. An optimal response is defined as $\leq$10% BCR-ABL1 transcripts at 3 months (1-log reduction), <1% at 6 months (2-log reduction), and $\leq$0.1% at 12 months (3-log reduction). If these milestones are not achieved, it may indicate treatment failure, and prompt a recommended switch to a different TKI. Cytogenetically, a partial cytogenetic response (PCyR; 1%-35% Ph$^+$ metaphases) at 3 months and a complete cytogenetic response (CCyR; no Ph$^+$ metaphases) by 6 months define an optimal response (Baccarani *et al.,* 2009).

Molecular monitoring of the disease by qRT-PCR is generally favoured over cytogenetics because it is simpler to perform and only requires a blood draw as opposed to a BM biopsy. However, it is recommended that both cytogenetic and molecular tests are performed until a CCyR and a major molecular response (MMR; 3-log reduction in BCR-ABL1 transcripts) are achieved (Baccarani *et al.,* 2013). Despite the fact that some TKI-responding patients have undetectable levels of BCR-ABL1 transcripts, designated as

complete molecular remission, the European LeukemiaNet guidelines recommend that patients continue treatment indefinitely. However, this may not be possible for some patients, particularly in the United States, where IM costs $146,000 per year (as of 2016) (Kantarjian, 2016).

Outcomes for many CML patients on TKIs have been incredibly positive, and deep molecular responses (reduction of BCR-ABL1 transcript levels by > 3-logs) have been possible in many patients. Consequently, there has been interest in studying the effects of discontinuation of TKI therapy. A study undertaken by Mahon and colleagues, the STop IMatinib (STIM) study, reported that in patients that had maintained complete molecular remission for at least two years, 39% did not relapse within 12 months. However, the other 61% did (Mahon *et al.,* 2010), indicating that, despite undetectable levels of BCR-ABL1 transcripts, LSCs had still persisted and were able to reconstitute the malignancy. The results highlight the necessity for therapies that can selectively target LSCs. One suggested approach has been the use of combination therapies – one drug to target the LSCs, and a TKI to target the mature leukemic cells, which constitute the bulk of the malignancy. One method to target TKI-resistant LSCs is to inhibit other pro-survival signaling pathways that are crucial to these cells, besides those controlled by BCR-ABL1. One possible mechanism is through the inhibition of the Hedgehog pathway.

1.2   The Hedgehog Signaling Pathway

1.2.1   Introduction of Key Proteins in the Hedgehog Pathway

The Hedgehog (HH) gene was first described in *Drosophila melanogaster* in 1980 as the result of a genetic screen (Nusslein-Volhard & Wieschaus, 1980). The larval mutants that were *hh* null had a lawn of disorganized denticles on their ventral surface that resembled hedgehog spines. The HH pathway is critical for pattern formation in the developing embryo as well as adult homeostasis (reviewed in Petrova & Joyner, 2014). The initiator of the pathway is the HH ligand. In mammals, there are three HH proteins: Indian Hedgehog (IHH), Desert Hedgehog (DHH), and Sonic Hedgehog (SHH); all of which seem to have distinct expression patterns with few overlapping roles (Bitgood & McMahon, 1995; Hammerschmidt *et al.,* 1997). IHH is involved in early hematopoiesis (Dyer *et al.,* 2001) and skeletal development (St. Jacques *et al.,* 1999); whereas DHH plays a role in spermatogenesis (Bitgood *et al.,* 1996). Lastly, SHH is the best studied HH homolog and is critical for the establishment of the lateral-medial (left-right) axis in the mouse embryo (Tsukui *et al.,* 1999), ventral cell fates in the central nervous system (Ericson *et al.,* 1997), and antero-posterior limb development (Riddle *et al.,* 1993). However, although these different ligands regulate the formation of diverse structures, their mode of action appears to be the same.

These secreted ligands bind to and inactivate a 12-pass transmembrane protein called Patched (PTCH) through a direct palmitate-dependent interaction (Tukachinsky *et al.,* 2016). HH ligand binding prevents the action of PTCH, which is involved in the constitutive inactivation of the transmembrane protein called Smoothened (SMO), a member of the G protein-coupled receptor superfamily. Although the precise mechanism of SMO inhibition by PTCH still remains unclear, it is known that PTCH contains a sterol-sensing domain and is structurally similar to members of the RND transporter family (Tseng *et al.,* 1999). It has been

demonstrated that mutations in the RND permease motif of PTCH diminish the repression of SMO (Taipale *et al.,* 2002), suggesting that PTCH may control the influx or efflux of a molecule that regulates SMO. In addition, many natural and synthetic SMO agonists and antagonists are structurally related to sterols (Ruat *et al.,* 2014). Taken together, it is plausible that PTCH regulates SMO by transporting a sterol-like ligand across the membrane, and that this ligand either activates or represses SMO.

Downstream of SMO, the roles of the key intracellular mediators of the pathway have yet to be completely delineated in vertebrates; however, it is understood that the primary cilium is an essential organelle that facilitates this process (Goetz & Anderson, 2010). Upon HH pathway activation, SMO accumulates at the basal body of the primary cilium via interactions with β-arrestin and KIF3A (Chen *et al.,* 2004; Kovacs *et al.,* 2008). Simultaneously, the ultimate effectors of the pathway, the glioma-associated (GLI) zinc finger transcription factors are found at the tip of the primary cilium in complex with a repressive protein called Suppressor of Fused (SUFU) (Wen *et al.,* 2010). In the presence of HH ligand, GLI-SUFU complexes dissociate, and full-length, activated GLI proteins translocate to the nucleus and turn on HH pathway target genes involved in proliferation (Kenney *et al.,* 2003) and cell cycle progression (Kenney & Rowitch, 2000). This includes the induced expression of the negative regulator PTCH, as well as the GLI genes themselves, suggesting a very tightly regulated feedback loop (Figure 1.3A). However, in the absence of HH ligands, GLI remains bound to SUFU, which promotes the phosphorylation and subsequent proteolytic processing of GLI to a repressive form (GLIR). GLIR translocates to the nucleus and prevents to transcription of HH pathway targets (Niewiadomski *et al.,* 2014) (Figure 1.3B).
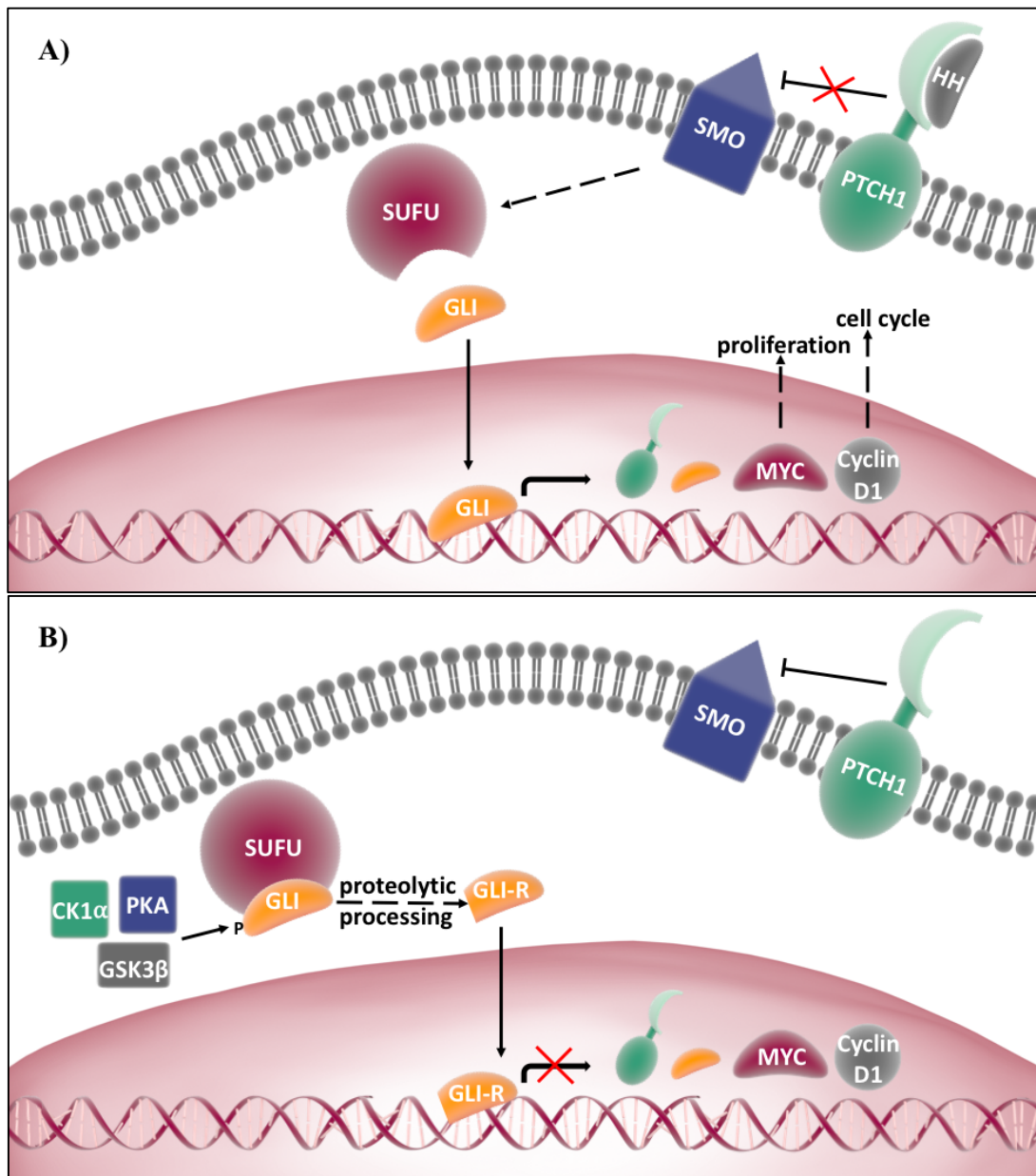
Figure 1.3   **Hedgehog signaling in vertebrates. A)** In the presence of HH ligand, PTCH1 cannot inactivate SMO. SMO is internalized and traffics to the primary cilium concurrently with SUFU/GLI complexes, which stimulates the dissociation of GLI from SUFU. Full-length GLI proteins translocate to the nucleus and turn on HH pathway genes. **B)** In the absence of HH, PTCH1 inactivates SMO, preventing its accumulation at the primary cilium. GLI remains bound to SUFU and is phosphorylated by CK1α, PKA, and GSK3β, which promotes proteolytic processing by the proteasome. The cleaved and repressive GLI-R isoform translocates to the nucleus and prevents the transcription of HH pathway targets.

1.2.2 Role in Development

The HH pathway plays many diverse roles in development. HH ligands can act as morphogens, mitogens, or differentiation factors, depending on the cellular context (Kenney *et al.,* 2003; Dessaud *et al.,* 2008; Saldana *et al.,* 2016). SHH is detected as early as E9.5 in the mouse embryo, equivalent to approximately the 3rd week of human development, and in the region of the notochord (Echelard *et al.,* 1993). In this context, SHH acts as a morphogen. Its secretion establishes a concentration gradient along the ventral neural tube which regulates the expression of transcription factors. A transcriptional code according to this concentration gradient demarcates spatially distinct progenitor domains, which in turn inform ventral CNS cell fates (Lupo *et al.,* 2006).

During odontogenesis, SHH acts as a mitogen. SHH is produced and secreted by dental epithelium, acting in an autocrine manner by enhancing epithelial cell proliferation. It also comes in contact with the underlying mesenchyme, in a paracrine manner, to stimulate tooth germ growth (Wu *et al.,* 2003). In addition, SHH can act as a differentiation factor in embryonic stem (ES) cell and induced pluripotent stem (iPS) cell models of Parkinson's disease (Cooper *et al.,* 2010). Specifically, the addition of SHH promotes the differentiation of ES and iPS cells to $FOXA2^{+}$ neural progenitor cells (NPC), and the sequential addition of other factors directs differentiation of NPCs to dopaminergic neurons.

1.2.3 Role in Congenital Syndromes and Cancer

The consequence of mutations in different HH pathway members is often redundant, depending on whether the overall effect of the mutation suppresses or enhances pathway

activity. In addition, the timing and location of the mutation in the greater tissue context also informs the overall consequence to the organism. The role of the HH pathway in human disease was first described in 1996 when inherited inactivating mutations in *SHH* were linked with holoprosencephaly (HPE), a midline defect involving the development of the forebrain and midface (Roessler *et al.,* 1996). Inactivating mutations in *GLI2* and *PTCH1* are also associated with HPE (Ming *et al.,* 2002; Roessler *et al.,* 2003). In addition, mutations in *GLI3* can give rise to three distinctive congenital anomalies: Greig cephalopolysndactyly syndrome, Pallister-Hall syndrome, and Postaxial polydactyly type A1. Greig syndrome is characterized by hypertelorism, preaxial or postaxial polydactyly, and syndactyly. Point mutations, large deletions, and translocations around the zinc-finger domain of *GLI3* have been described in Greig syndrome patients (Kruger *et al.,* 1989; Wild *et al.,* 1997; Demurger *et al.,* 2015). Pallister-Hall syndrome patients have postaxial polydactyly, anal abnormalities, and hypothalamic hamartomas. Frameshift mutations downstream of the zinc-finger domain of *GLI3,* leading to premature truncation of the protein, have been described in patients (Kang *et al.,* 1997). Postaxial polydactyly type A1 is inherited in an autosomal dominant fashion and is characterized by the presence of a well-formed and functional supernumerary digit. It is associated with mutations closer to the C-terminus of the GLI3 protein (Radhakrishna *et al.,* 1997).

Alternatively, inherited mutations that lead to hyperactivation of the pathway often predispose to cancer. Indeed, gain-of-function mutations in *SHH* contribute to the formation of basal cell carcinoma (Oro *et al.,* 1997). Also, heterozygous loss-of-function mutations in *PTCH1* cause Gorlin syndrome or basal cell nevus syndrome, which is characterized by

skeletal abnormalities, increased frequency of basal cell cancers, and other neoplasms including medulloblastoma (Gorlin, 2004). HH pathway activation has also been described as a driver in different forms of cancer, including pancreatic (Thayer *et al.,* 2003), breast (Kubo *et al.,* 2004), small cell-lung cancer (Watkins *et al.,* 2003), gastric adenocarcinoma (Ma *et al.,* 2005), AML (Wellbrock *et al.,* 2015) and CML (Dierks *et al.,* 2008; Zhao *et al.,* 2009).

1.2.4   Role in CML

The role of the HH pathway in CML was not appreciated until two landmark papers were published in 2008 and 2009. Dierks and colleagues and Zhao and colleagues, respectively, demonstrated that intact HH signaling was required for CML LSC maintenance.

In the Dierks *et al.* study, they observed that homozygous loss of *SMO* in mouse fetal HSCs retrovirally transduced with BCR-ABL1/GFP had an impaired ability to cause leukemia when injected into immunodeficient mice. Indeed, disease latency was increased by more than three months in this group compared to wild-type controls, and only 60% of recipients developed any lethal disease. To further investigate the effects of HH signaling in the LSC compartment, BM from the diseased mice was collected and re-transplanted into secondary hosts. No mice receiving *SMO$^{-/-}$* BCR-ABL1/GFP^{+} cells developed leukemia, compared with controls, who developed leukemias within two months after secondary transplantation.

Next they tested a pharmacological inhibitor of SMO called cyclopamine in combination with AMN *in vitro* and *in vivo* and observed that the combination was superior to a TKI alone in reducing the *in vitro* colony-forming ability of CML stem and progenitor cells from patients, and in decreasing spleen and liver weights in mice. Overall, the results obtained

by Dierks and colleagues supported the hypothesis that intact HH signaling, mediated by SMO was essential for the expansion of LSCs both *in vitro* and *in vivo.*

Less than one year later, *Zhao et al.* published a similar study investigating the effects of SMO inhibition on CML cell initiation and maintenance. Using a conditional knockout mouse model in which *SMO* was selectively deleted in hematopoietic cells, they observed that mice injected with retrovirally-transduced BCR-ABL1/GFP$^+$ primitive (Lin$^-$Sca-1$^+$c-Kit$^+$, LSK) mouse BM cells survived significantly longer than mice with intact *SMO* (94% recipients with intact *SMO* had CML within 3 months vs 47% in *SMO*-deficient mice). In addition, *SMO$^{-/-}$* mice had significantly fewer BCR-ABL1/GFP$^+$ LSK cells in the BM compared to mice with wild type SMO (2% vs 8%, $p<0.01$). In a similar experiment, leukemic mice were treated with cyclopamine, a pharmacological inhibitor of SMO, and the treated mice survived significantly longer than controls (60% treated mice were alive after 7 weeks whereas all control animals succumbed to a CML-like disease within 4 weeks) and had significantly fewer BCR-ABL1/GFP$^+$ LSK cells in their BM (1% vs 14%, $p<0.05$). These results suggested that HH activity is required for the maintenance of LSCs. Taken together with the results from the Dierks *et al.* study, they raised the possibility that the HH pathway, and particularly SMO, may be a therapeutic target for drug-insensitive CML LSCs.

1.3   Summary

The persistence of LSCs remains a significant barrier to achieving cures in CML patients. Great effort has been invested in uncovering alternative mechanisms that LSCs exploit to evade eradication by TKIs. One such mechanism is the activation of HH signaling,

an important pathway during early embryonic development that has recently been described to play a role in LSC maintenance in CML mouse models (Dierks *et al.,* 2008; Zhao *et al.,* 2009). An attractive therapeutic strategy, therefore, would be the use of a TKI to target the bulk of the mature leukemic cells in combination with HH pathway suppression, through the inhibition of SMO, to eradicate the CML LSCs. However, the extent to which the HH pathway is activated in CML patients is unknown, particularly between IM responders and IM non-responders, and a better understanding of the reliance of human CML LSCs on HH signalling is clearly needed.

1.4   Hypotheses

1)   The HH pathway is critical for the survival of primitive CML cells.

2)   Inhibition of the HH pathway in addition with a TKI, may provide a more effective therapeutic effect on primitive CML cells.

1.5   Thesis Objectives

1)   Investigate the expression of HH pathway genes in HBM controls and CML patient samples, and in different hematopoietic cell populations;

2)   determine how ABL1 inhibitor BOS and SMO inhibitor PF913 affect different populations of CML cells alone, and in combination;

3)   demonstrate that SMO inhibition via PF913 results in the decreased expression of HH pathway target genes.

CHAPTER 2 MATERIALS AND METHODS

2.1 Cell Culture

2.1.1 Patient Samples

Heparin-anticoagulated PB or BM cells were collected from healthy donors and CML patients at diagnosis, prior to the initiation of TKI therapy. Informed consent was obtained in accordance with the Declaration of Helsinki and all procedures were approved by the University of British Columbia Clinical Research Ethics Board (certificate number H12-02372). Mononuclear cells were isolated using Ficoll-Paque density gradient separation and CD34$^+$ cells were enriched using the EasySep™ Human CD34 Positive Selection Kit (STEMCELL Technologies). Purity was verified by staining isolated cells with an anti-CD34 antibody conjugated to allophycocyanin (APC) (BD BioSciences, Mississauga, ON) followed by flow cytometry on a FACSCalibur™ cytometer (BD Biosciences) and analysis by FlowJo® 10 software. A purity of at least 85% CD34$^+$ cells was considered acceptable.

Purified CD34$^+$ cells were cultured in serum-free medium consisting of Iscove's Modified Dulbecco's Medium (MDM) with BIT 9500 Serum Substitute supplemented with human growth factors (20 ng/mL IL-3, 20 ng/mL IL-6, 100 ng/mL Flt3 ligand, and 20 ng/mL G-CSF) (all from STEMCELL Technologies).

Samples were obtained from newly diagnosed patients that were retrospectively characterized as either IM responders or IM non-responders according to the European LeukemiaNet CML treatment guidelines (Baccarani *et al.,* 2013). IM responders were defined as individuals who achieved at least a 3-log reduction in BCR-ABL1 transcript levels after 12

months using qRT-PCR. CCyR was defined by the absence of Ph$^+$ cells detected by cytogenetic analysis or FISH at 6 months. IM non-responders were classified as those that did not meet these criteria or that subsequently lost an initial response.

Table 2.1   Clinical information for CML patient samples

Patient number	Sex	Age at Diagnosis	WBC at Diagnosis ($\cdot 10^3$/mL)	Disease Stage at Diagnosis	IM Response
CML 1	M	45	392.3	CP-CML	NR
CML 2	M	22	212.8	CP-CML	NR
CML 3	M	N/A	N/A	CP-CML	NR
CML 4	F	66	492.0	CP-CML	NR
CML 5	M	55	676.6	CP-CML	NR
CML 6	M	48	140.0	CP-CML	NR
CML 7	M	21	202.9	CP-CML	NR (BC)
CML 8	M	24	88.7	CP-CML	NR
CML 9	F	19	355.5	CP-CML	NR
CML 10	M	28	225.5	CP-CML	NR (non-compliant)
CML 11	M	27	480	CP-CML	NR
CML 12	F	N/A	197	CP-CML	NR
CML 13	M	42	244.2	CP-CML	NR
CML 14	F	56	301.6	CP-CML	R
CML 15	M	23	324.4	CP-CML	R
CML 16	F	78	192.3	CP-CML	R
CML 17	M	N/A	N/A	CP-CML	R
CML 18	M	32	353.2	CP-CML	R
CML 19	M	57	450	CP-CML	R
CML 20	M	54	77	CP-CML	R
CML 21	M	59	37.6	CP-CML	R

N/A = not applicable, patient information not available

2.1.2   Inhibitors

BOS and PF-04449913 were obtained from Pfizer (New York, NY) and reconstituted from powder in 100% DMSO. Drugs were stored at -20°C as 10 mM stock solutions. Working

solutions were made by diluting the stock solution 1/10 in 40% DMSO in Iscove's MDM. Subsequent dilutions, if necessary, used Iscove's MDM alone.

2.1.3   Fluorescence-Assisted Cell Sorting

Primary mononuclear PB or BM cells were isolated and washed with Hank's Balanced Salt Solution (HBSS) (STEMCELL Technologies) with 2% FBS. Cells were then stained with anti-human CD38-FITC and CD34-APC antibodies (both from BD Biosciences) and incubated on ice for 30-45 minutes. Cells were then washed with HBSS with 2% FBS and 1 µg/mL PI and filtered. CD34$^+$ subpopulations were sorted as described previously (Jiang *et al.,* 2007) and used for experimental applications.

2.2   Molecular Techniques

2.2.1   RNA Extraction

Total RNA was extracted using TRIzol® (ThermoFisher Scientific, Burlington, ON) according to the manufacturer's instructions. 10 µg RNase-free glycogen was added as a carrier to assist with the visualization of the RNA pellet. Purified RNA was diluted in UltraPure™ DNase/RNase-free distilled water (ThermoFisher Scientific, Burlington, ON) and stored at -80°C. RNA purity was determined by the A260/A280 optical density (OD) ratio and the RNA concentration was measured using a NanoDrop™ spectrophotometer (ThermoFisher Scientific, Burlington, ON).

2.2.2   RNA Sequencing and Bioinformatic Analysis

1 µg total RNA was isolated from CD34$^+$ cells isolated by FACS from 3 healthy BM (HBM) control samples, 3 IM responder CP-CML patient samples, and 3 IM non-responder

CP-CML patient samples. Polyadenylated mRNA was purified using the MultiMACS mRNA Isolation Kit (Miltenyi Biotec, Auburn, CA) and cDNA was synthesized using the Maxima H Minus First Strand cDNA Synthesis Kit (ThermoFisher Scientific). cDNAs were amplified using the Illumina PE primer set and paired-end sequenced on the HiSeq 2000 platform (Illumina, San Diego, CA) at the BC Genome Sciences Centre (Vancouver, BC).

The resulting sequence data was aligned to GRch37-lite genome-plus-junctions reference using the Burrows-Wheeler Aligner and human reference genome version 10 coordinates (Li *et al.,* 2009; Butterfield *et al.,* 2014). Raw read values were expressed as reads per kilobase of transcript per million mapped reads (RPKM) and coverage was determined by summing the sequence reads for protein-coding genes, pseudogenes, processed transcripts, and other non-coding RNAs.

Differential gene expression between HBM controls and CP-CML samples was quantified using *DESeq2* analysis (Love *et al.,* 2014). To minimize a high false discovery rate, p-values were adjusted using the *Benjamini-Hochberg (B-H)* method (Benjamini & Yekutieli, 2001).

2.1.3   Quantitative Reverse Transcription Polymerase Chain Reaction

100-200 ng RNA was reverse transcribed into cDNA using the Superscript® VILO cDNA Synthesis Kit (ThermoFisher Scientific) according to the manufacturer's instructions. The resulting cDNA was then diluted 1/10 in ddH_2O. qRT-PCR was performed with 1X SYBR Green PCR Master Mix (ThermoFisher Scientific), 50% v/v diluted cDNA, and 5 nmol each of the forward and reverse primers in a 96-well plate using a 7500 Real Time PCR System (ThermoFisher Scientific). SYBR was used as the reporter dye and ROX as the passive

reference. Gene expression was quantified using the ΔΔCt method with *β2-microglobulin* (*β2M*) as the housekeeping control gene. Primers used are listed in Table 2.2.

Table 2.2   Specific primer sequences for qRT-PCR

Primer	Sequence (5′→3′)
β2M-F	TAGCTGTGCTCGCGCTACT
β2M-R	TCTCTGCTGGATGACGTGAG
PTCH1-F	CCACAGAAGCGCTCCTACA
PTCH1-R	CTGTAATTTCGCCCCTTCC
SMO-F	TTACCTTCAGCTGCCACTTCTACG
SMO-R	GCCTTGGCAATCATCTTGCTCTTC
GLI1-F	TTCCTACCAGAGTCCCAAGT
GLI1-R	CCCTATGTGAAGCCCTATTT
GLI2-F	GGATTCCAGCTGTCTTGTCTT
GLI2-R	CCAGAGAGGATGCCCATAAAC

2.3   Biological Assays

2.3.1   Viability Assay

1.2×10^4 CD34$^+$ CML cells were seeded in Falcon® 96-well round-bottom tissue culture plates (Corning) containing 100 μL serum-free medium with growth factors ± inhibitors, and cell viability was assessed after 72 hours using the trypan blue exclusion method. Total viable cell numbers were determined using a Neubauer hemocytometer and expressed as a percentage relative to untreated controls.

2.3.2   Apoptosis Assay

To quantify cell apoptosis, the Annexin V Apoptosis Detection Kit APC (eBioscience, San Diego, CA) was used according to the manufacturer's instructions. Cells were harvested after 72-hour exposure to inhibitors and stained with an Annexin V-APC antibody and PI. Flow cytometry analysis was performed and the proportion of apoptotic cells was determined

by summing "early" (Annexin V^+/PI^-) and "late" apoptotic (Annexin V^+/PI^+) cell subpopulations. This number was expressed as a percentage above the amount of apoptosis in untreated controls, in order to account for the variability in the level of basal apoptosis between primary patient samples.

2.3.3 CFC Assay

10^3 CD34$^+$ cells ± inhibitors were plated in duplicate 35 mm cultures dishes (STEMCELL Technologies) per 1 mL of MethoCult™ H4230 (STEMCELL Technologies) medium with growth factors (20 ng/mL IL-3, 20 ng/mL IL-6, 50 ng/mL G-CSF, 50 ng/mL GM-CSF, and 2 U/mL EPO, all from STEMCELL Technologies). After a 12-14-day incubation at 37ºC and 5% CO_2, erythroid, granulopoietic, and mixed colonies were enumerated and the numbers of test arms expressed as a percent of the numbers measured in parallel untreated control assays (Hogge *et al.,* 1996). Mixed colonies (GEM; granulocyte/ erythroid/macrophage) composed a very small proportion of the total colony number (never more than two colonies in any given assay), so I decided to remove them from all figures.

To investigate the effect of drugs on more primitive hematopoietic cells, the resulting colonies from the CFC were isolated, individual cells counted, and 10^4 cells per 1 mL of MethoCult™ H4230 with growth factors and without drugs were re-plated in duplicate. Colonies were scored 7 days later in the same manner as above. The CFCs derived from the re-plating experiment were expressed as a percent of the total number of cells harvested at the end of the 2-week replating experiment, and back calculated per the original input of 10^3 cells per 1 mL MethoCult™ into the initial CFC. The resulting value from the untreated control was

considered 100%, that is, no change in re-plating potential because there was no treatment. All values from the treatment arms were expressed as a percentage of the untreated control.

2.3.4 Long-term Culture-Initiating Cell (LTC-IC) Assay

To investigate the effect of inhibitors on primitive leukemic stem cells, the LTC-IC assay was utilized (Hogge *et al.,* 1996). 2×10^4 CD34$^+$ cells were cultured for 6 weeks in MyeloCult™ H5100 medium (STEMCELL Technologies) in Falcon® 24-well flat bottom cell culture plates on a mix of 2 irradiated mouse stromal cell lines that have been genetically engineered to secrete human growth factors (IL-3, G-CSF, and stem cell factor; kindly provided by Dr. C. Eaves, BC Cancer Agency, Vancouver). Inhibitors were added at the outset of the experiment, and one half medium changes were performed once per week without the addition of inhibitors. After 6 weeks, the cells were harvested and 10^4 viable cells per 1 mL Methocult™ H4230 with growth factors were plated in CFC assays as described above. Results were calculated by dividing the number of CFC colonies by the number of cells plated into the CFC. This value was then multiplied by the total number of cells harvested from the liquid culture after six weeks and then divided by the original input of 2×10^4 cells. Similar to the CFC, all values were expressed as a percentage and normalized to the untreated control.

CHAPTER 3 RESULTS

3.1   Identification of differentially expressed HH pathway-associated genes in CD34$^+$ CML cells compared with HBM controls

RNA sequencing (RNA-seq) was performed on three CD34$^+$ HBM controls and six CD34$^+$ CML patient samples obtained at diagnosis. The differential expression of 42 HH pathway-associated genes (Briscoe & Therond, 2013; Kanehisha *et al.,* 2017) was investigated using Bioconductor *DESeq2* analysis (Love *et al.,* 2014). Of the 42 genes investigated, 17 were significantly (*Benjamini-Hochberg*-adjusted p-value<0.05) differentially expressed (-0.58<log$_2$ fold change>0.58; corresponds to 1.5-fold) in CD34$^+$ cells from the CML samples compared with HBM controls (Table 3.1). For these, transcript levels of 10 genes were decreased in the CML samples and 7 genes were increased. In particular, transcripts for one of the principal HH pathway genes, *GLI2,* were particularly elevated in the CD34$^+$ CML cells (67-fold, p=1.11×10^{-18}, Figure 3.1). In addition, *SMO* transcripts were higher (1.7-fold), transcripts of the negative-regulator *PTCH1* were slightly lower (1.6-fold), and transcripts of *GLI1* were significantly reduced (4.3-fold, p=1.73×10^{-5}). These results suggest that the HH pathway is more active in CD34$^+$ CML cells compared with CD34$^+$ cells from HBM.
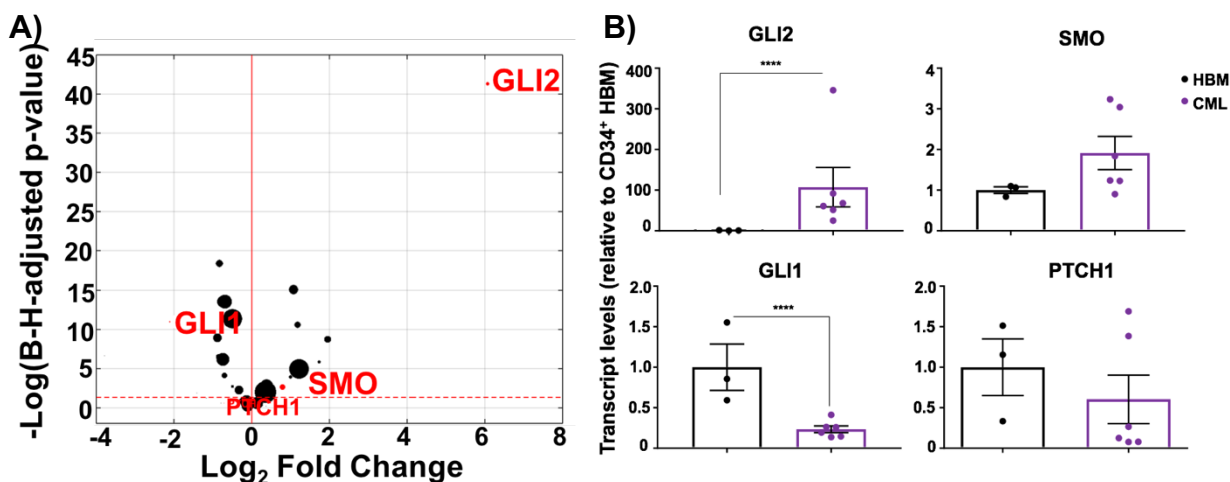
Figure 3.1 Identification of differentially expressed HH pathway-associated genes in CD34$^+$ CML cells compared with HBM controls. A) Volcano plot demonstrating differential gene expression of 42 HH pathway-associated genes between CD34$^+$ CML patient samples (n=6) and HBM controls (n=3) by Bioconductor *DESeq2* analysis. The principal HH pathway genes are highlighted in red. The size of the dots corresponds to mean expression level in absolute read counts and normalized for sequencing depth. The broken red line demarcates the threshold of significance (Benjamini-Hochberg-adjusted p-value < 0.05). **B)** Expression of the principal HH pathway genes between HBM and CML quantified in RPKM. **** = p<0.0001. The RNA-seq experiment and *DESeq2* analysis was performed by Dr. Hanyang Lin in collaboration with Dr. Ryan Brinkman of the Terry Fox Laboratory, BC Cancer Agency. I extracted the results for the relevant genes and Robert Izett, UBC, created Panel A.

Table 3.1   Differential expression of 42 HH pathway-associated genes between 3 CD34$^+$ HBM and 6 CD34$^+$ CML samples by RNA-seq analysis

Gene Name	Sequencing Mean Expression (absolute normalized read count)	Fold Change (log$_2$)	Benjamini-Hochberg Adjusted p-value
GLI2	630	6.1	1.11E-18
KIF3B	2500	-0.83	1.05E-08
ARRB1	4100	1.1	2.80E-07
CUL3	9000	-0.69	1.30E-06
NUMB	6300	-0.75	1.35E-06
CSNK1A1	17000	-0.50	1.19E-05
GLI1	76	-2.1	1.73E-05
STK36	1900	1.2	2.57E-05
FBXW11	3500	-0.88	0.00013

Gene Name	Sequencing Mean Expression (absolute normalized read count)	Fold Change (log$_2$)	Benjamini-Hochberg Adjusted p-value
EVC	2200	2.0	0.00016
BOC	5.4	-3.8	0.00138
SUFU	1700	-0.84	0.00150
GSK3B	7700	-0.75	0.00212
CCND1	510	1.7	0.00293
MYC	18000	1.2	0.00694
KIF7	1500	-0.71	0.01638
EVC2	560	1.0	0.01992
GLI4	630	0.35	0.04043
PRKACA	2800	0.32	0.05779
LRP2	66	1.1	0.05804
BMI1	8400	0.38	0.06114
PTCH2	370	-0.50	0.06701
SMO	1500	0.79	0.07276
ARRB2	3500	-0.32	0.10527
PRKACB	22000	0.35	0.13193
IHH	5.1	-1.4	0.15359
KIF3A	970	0.27	0.25332
BCL2	3400	0.35	0.28759
CDO1	8.2	-1.2	0.29298
KIF3C	2000	-0.25	0.43424
CUL1	7600	-0.13	0.46816
GLI3	120	1.0	0.51055
PTCH1	38	-0.72	0.53682
DHH	6.2	-0.79	0.54207
HIP1	6800	0.14	0.56271
SPOPL	6700	-0.11	0.74558
GPR161	340	-0.17	0.75306
GAS1	36	0.36	0.79083
SHH	2.8	0.029	0.98689
PRKACG	0.19	0.12	NA
HHIP	230	-6.9	NA
IGF2	77	-7.6	NA

3.2 Several key genes in the HH pathway are differentially expressed in CD34$^+$ cells from IM non-responders compared to IM responders

Next, gene expression differences between IM responder and IM non-responder patient samples were compared using RNA-seq analysis. Of the six CD34$^+$ CML patient samples used for the experiment, three were retrospectively characterized as IM responders, and three were non-responders. In general, the variation in expression was high in all of the investigated genes, which precluded most of the genes from reaching statistical significance (Table 3.1). Of the four principal HH pathway genes (*SMO, GLI2, GLI1, PTCH1*), transcripts for *GLI1* were marginally significantly more decreased in IM responders than in non-responders (Figure 3.2A) but for *PTCH1* were not different. *SMO* transcripts were slightly higher in IM responder patient samples (1.4-fold relative to HBM), and even more so in IM non-responders (2.4-fold relative to HBM). *GLI2* transcripts followed a similar, yet more striking pattern to *SMO* transcripts in being more elevated in IM responders (48-fold relative to HBM), and even more so in IM non-responders (166-fold relative to HBM; 3.5-fold relative to IM responders).

To further test these RNA-seq results, qRT-PCR was performed in more patient samples. The results of these measurements generally mirrored those obtained by RNA-seq (Figure 3.2B). Specifically, *GLI2* transcripts were significantly higher in CD34$^+$ cells from IM non-responders compared to those from IM responders (4-fold, $p<0.05$), and significantly higher in CD34$^+$ cells from IM non-responders compared to those from HBM (60-fold, $p<0.01$). *SMO* transcripts followed a similar pattern (higher in IM non-responder cells compared to IM responders (2.6-fold, $p<0.05$), and significantly higher in IM non-responder
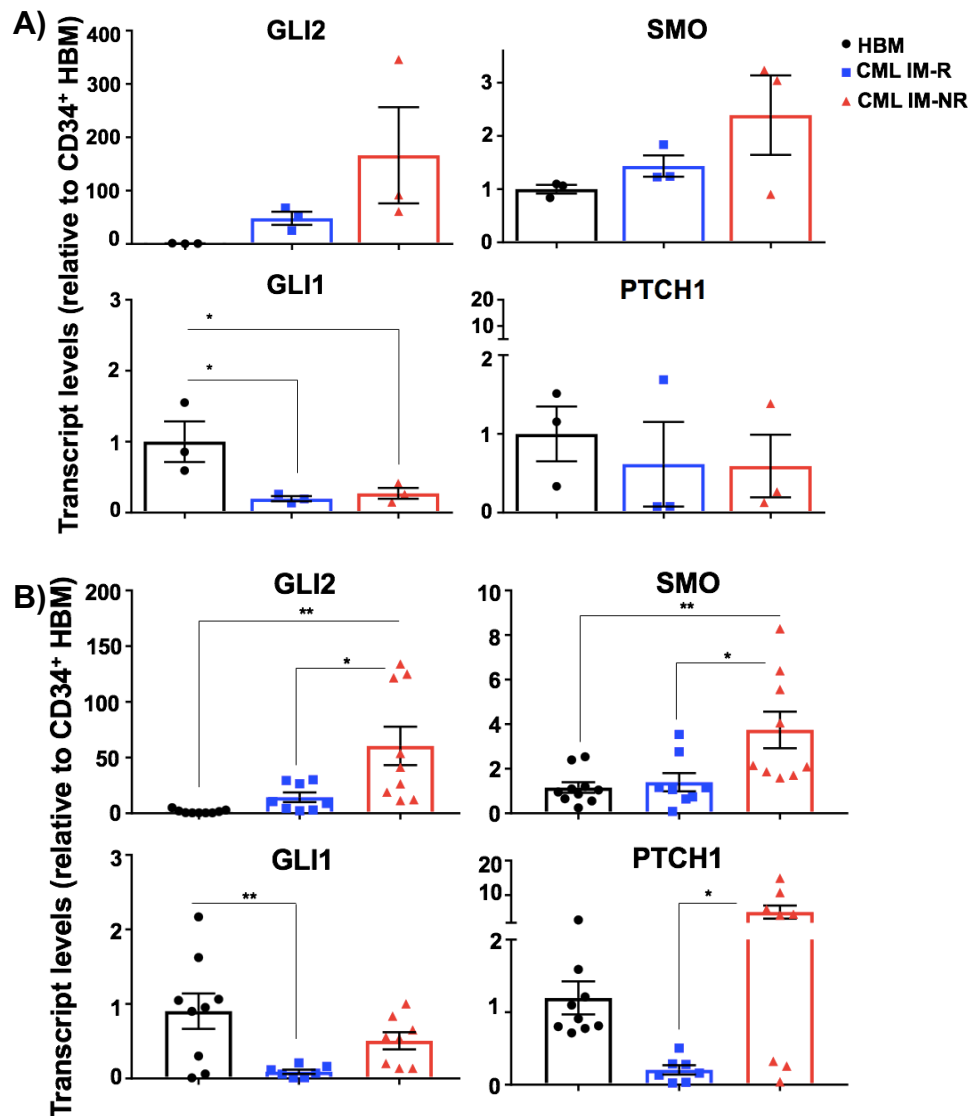
Figure 3.2 **Several key HH pathway genes are differentially expressed in CD34$^+$ cells from IM non-responders compared with IM responders. A)** Expression of principal HH pathway genes relative to CD34$^+$ HBM cells (black bar, n=3) in IM responders (CML IM-R, blue bar, n=3) and IM non-responders (CML IM-NR, red bar, n=3) from RNA-seq. **B)** qRT-PCR validation on 8 CD34$^+$ HBM, 8 CD34$^+$ CML IM responders, and 9 CD34$^+$ CML IM non-responder samples. Individual values are shown as shapes and bars represent the mean $\pm$ SEM. (*=p<0.05; **=p<0.01). Statistical significance was determined by one-way ANOVA using the Bonferroni correction for multiple testing. From the raw RNA-seq files, I extracted the relevant gene expression information to make Panel A. I performed qRT-PCR on approximately half of the samples used for the validation study in Panel B, and the results from the remainder of the samples were provided by Dr. Katharina Rothe, Terry Fox Laboratory.

cells relative to HBM (3.6 fold, p<0.01). Taken together, these results suggest that the HH pathway may be more critical in regulating the properties of stem/progenitor cells from IM non-responder patients compared with IM responders.

3.3   The transcript levels of *GLI2* and *SMO* are more highly expressed in the more primitive CD34$^+$ CML cells

qRT-PCR analysis of HH pathway-associated gene expression in different subpopulations of CD34$^+$ was then also performed. Relative to CD34$^-$ CML cells, *GLI2* transcripts were highly increased in the Lin$^-$CD34$^+$38$^-$ (stem-enriched) fraction (38-fold), compared with the Lin$^-$CD34$^+$38$^+$ (progenitor) subpopulation (7-fold), and the difference between the stem-enriched fraction and the progenitors and mature cells was statistically significant (Figure 3.3, p<0.05). This effect was amplified when comparing the differences in *GLI2* expression in the different CD34-subpopulations between IM responders and IM non-responders. Compared with IM responders, IM non-responder cells expressed *GLI2* at a level >4-fold higher than in the stem-enriched subpopulation. A similar effect was seen, but to a lesser extent, in the other subpopulations from IM responders and non-responders.

SMO transcripts were also present at higher levels in the stem-enriched fraction relative to CD34$^-$ CML cells (10-fold), with a similar expression level seen in the progenitor subset as well. Again, this effect was exacerbated when comparing IM non-responders and IM responders, in that the non-responders expressed SMO in the stem/progenitor fractions to a greater extent than the IM responders (7-fold).
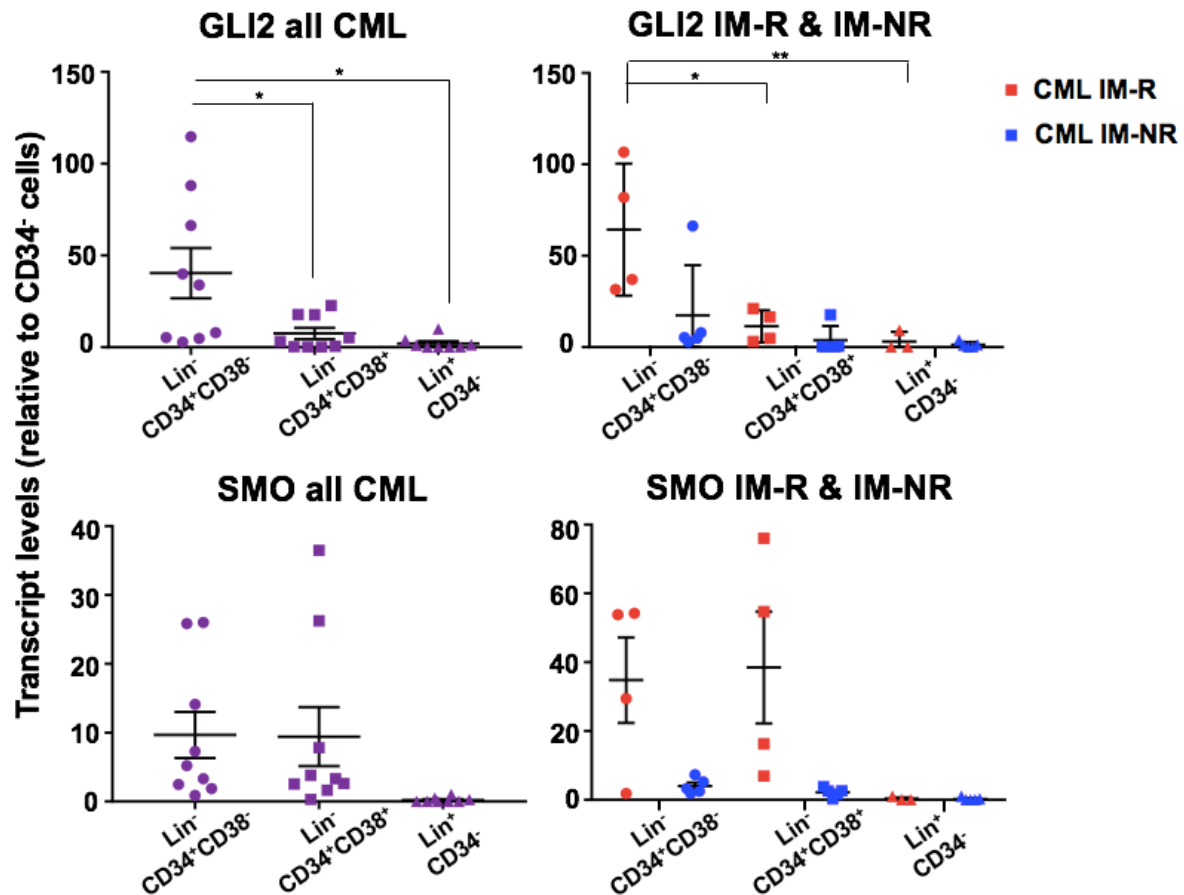
Figure 3.3 **Transcript levels of *GLI2* and *SMO* are higher in primitive hematopoietic cell subpopulations compared with more mature cells.** Relative *GLI2* and *SMO* expression by qRT-PCR in Lin⁻CD34⁺CD38⁻ stem-enriched subpopulation (circles), Lin⁻CD34⁺CD38⁺ progenitor subpopulation (squares), and Lin⁺CD34⁻ mature hematopoietic subpopulations (triangles). The first column from left (purple) demonstrates *SMO* and *GLI2* expression in all CML patient samples (n=9). The second column is expression in IM non-responders (n=5, red symbols) and IM responders (n=4, blue symbols). Each dot represents the relative expression of a particular patient sample with mean expression ± SEM also plotted. *=p<0.05, **=p<0.01. Statistical significance was determined by one-way ANOVA using the Bonferroni correction for multiple testing. Dr. Katharina Rothe sorted the cells and performed the qRT-PCR experiment and I generated the figure from the raw data.

These results demonstrate that both *SMO* and *GLI2* are most highly expressed in the stem-enriched subpopulation in both IM responder and IM non-responder CML patient samples, compared with more mature cell subsets. Most interestingly, they were more highly

expressed in the stem-enriched fraction from IM non-responder patient samples compared with IM responders, which may indicate that IM non-responders utilize the HH pathway as a pro-survival mechanism to evade eradication by TKIs.

3.4 CD34$^+$ cells from IM non-responders are more sensitive to SMO inhibition *in vitro* compared with IM responder cells

Next, I interrogated the effect of a highly selective SMO inhibitor, PF-04449913 (further referred to as PF913) on different CML cell populations. I first performed relatively short-term assays of CD34$^+$ cell viability and apoptotic responses. After 72 hours exposure, PF913 had a modest effect on the viability and apoptosis of CD34$^+$ cells from IM responders. Specifically, at doses up to 10 µM, viability decreased by 31% and apoptosis was induced in only 2% of cells (n=3, Figure 3.4A and B, blue bars). CD34$^+$ cells from IM non-responders showed a slightly greater decrease in cell viability (43% reduction), and more apoptosis (10%) compared with IM responders (n=3, Figure 3.4A and B, red bars). However, the differences between these two groups were modest and only marginally significant.

To examine the effects of SMO inhibition on more primitive leukemic cells, I tested PF913 on CD34$^+$ CML cells using the CFC assay. Compared with CD34$^+$ CML cells from IM responder patients (n=3), IM non-responders (n=3) were slightly more sensitive to PF913 (Figure 3.4C, 19% vs 10% reduction in colony formation relative to control assays without PF913). The drug did not appear to differentially target particular colony types in either IM responder or IM non-responder patient samples. All cells from the CFC assay were harvested and a proportion re-plated in fresh methylcellulose without drugs and enumerated 7 days later.

Re-plating interrogates a more primitive subset of leukemic progenitors that retain or have generated CFC capacity during the first two weeks in culture. PF913 did not have any effect on re-plated cells from IM responders, but resulted in a significant reduction in CFC yields from the primary re-plated assays compared with untreated control assays of the IM non-responder patient samples (2-fold, $p<0.01$, Figure 3.4D).

Overall, these results suggested that more primitive leukemic cells are more sensitive to SMO inhibition and that IM non-responders are more sensitive to SMO inhibition compared with IM responders. These results are in concordance with the gene expression data described in Chapter 3.2 and 3.3 and supported the hypothesis that the cell subsets that express key HH pathway genes to a greater extent are more sensitive to HH pathway inhibition.

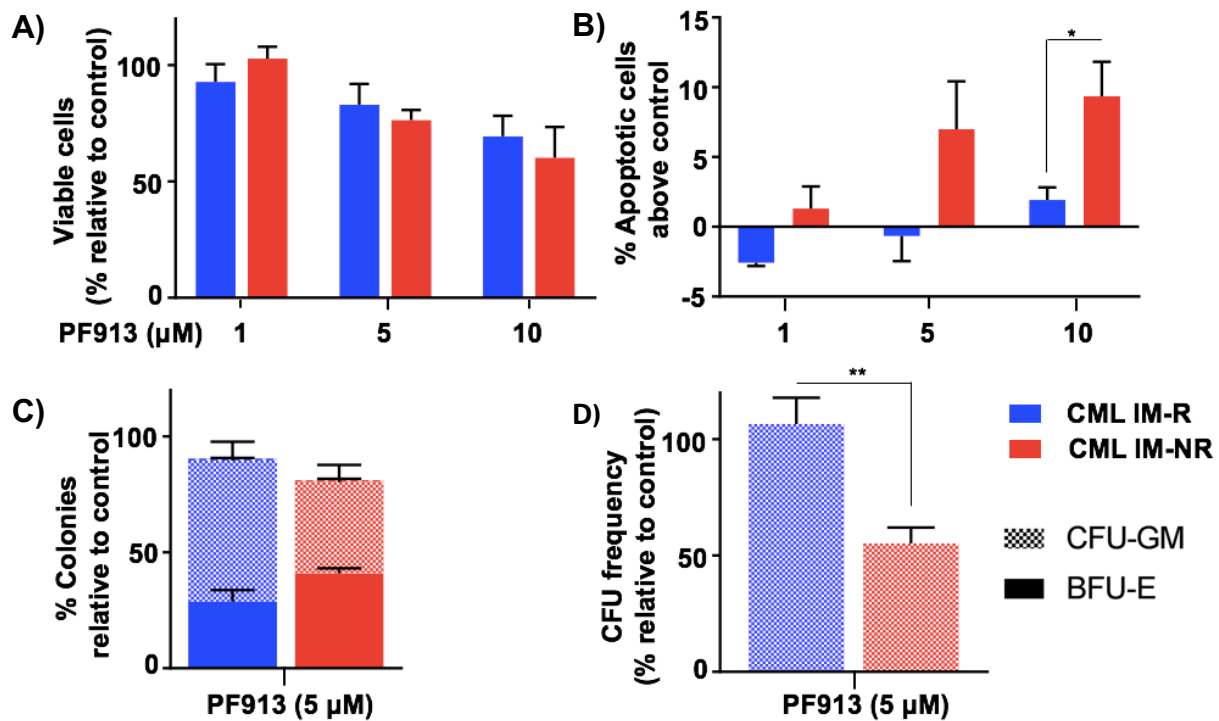**Figure 3.4   CD34⁺ cells from IM non-responders are more sensitive to SMO inhibition** *in vitro* **compared to IM responders. A)** Viability assay in CD34$^+$ cells after 72-hour exposure to increasing doses of PF-04449913 using trypan blue exclusion (n=3). **B)** Apoptosis assay in CD34$^+$ cells after 72-hour exposure to increasing doses of PF-04449913 using PI and Annexin V staining followed by FACS analysis (n=3) *=p<0.05. **C)** CFC assay (n=3). CD34$^+$ CML cells were plated in methylcellulose with growth factors ± inhibitors and colonies were enumerated and distinguished by type 14 days later **D)** CFC re-plating assay (n=3). A proportion of the cells from the CFC assay were harvested and re-plated into fresh methylcellulose with growth factors and no drugs. Colonies were enumerated and distinguished by type 7 days later. **=p<0.01. Blue bars represent IM responders and red bars represent IM non-responders. Bar patterns refer to colony-type based on morphology. BFU-E = burst-forming unit-erythroid, CFU-GM = colony-forming unit-granulocyte/ macrophage. Values represent mean ± SEM. Statistical significance was determined using a two-tailed Student's t-test. I performed all assays that contributed to this figure.

3.5 CD34$^+$ stem/progenitor cells from IM non-responders are sensitive to simultaneous SMO inhibition via PF913 and BCR-ABL1 via BOS

Since CD34$^+$ cells from IM non-responders were more sensitive to SMO inhibition compared with IM responders, and represent a more clinically interesting patient population, I decided to focus further experiments on IM non-responder patient samples. Viability, apoptosis, CFC, CFC re-plating, and LTC-IC assays were then performed in order to compare the effect of PF913 with a second generation ABL1 inhibitor, BOS on CD34$^+$ CML cells. I hypothesized that a combination approach might be more effective on IM-insensitive leukemic stem/progenitor cells compared to either agent alone. While primary CD34$^+$ CML cells did not appear to be very sensitive to PF913 alone (Figure 3.4A), reported IC$_{50}$s for BOS are in the low nanomolar range in BCR-ABL$^+$ cell lines (Puttini *et al.,* 2006; Keller-von Amsberg & Koschmieder, 2013) and in the low micromolar range for CD34$^+$ CFCs from CML patients (Konig *et al.,* 2008). In preliminary experiments with BOS alone at varying concentrations in CFC assays of 6 CML samples, I determined the IC$_{50}$ to be 2 μM (Figure 3.5.1), which is similar to the value previously reported (Konig *et al.,* 2008). In short-term (72-hour) viability assays, I observed an approximate 50% reduction in cell viability at approximately 0.5 μM BOS (Figure 3.5.2A).

In short-term (72-hour) viability and apoptosis assays, the drug combination was not superior to single agents in CD34$^+$ cells from three IM non-responder samples (Figure 3.5.2 A&B), and indeed, PF913 alone had no effect. In CFC assays, a significant decrease in colony number was observed in the combination treatment arm relative to single treatment with BOS

(n=3, Figure 3.5.2C, 54% vs 69% reduction, p<0.01), and colonies were almost completely

ablated upon re-plating in the combination treatment arm (11% colonies remaining),
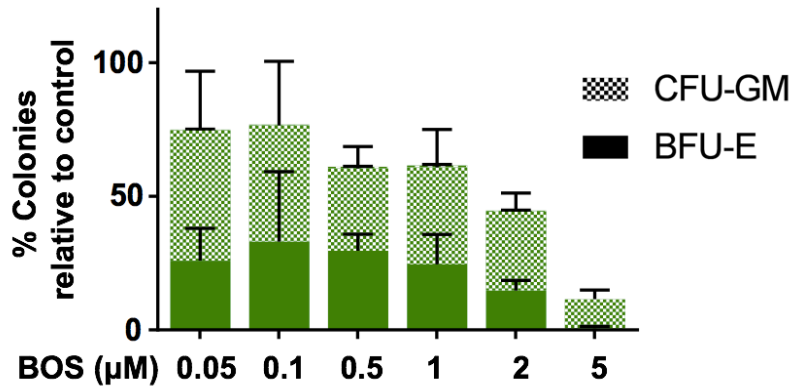
Figure 3.5.1   Optimization of BOS dose in CD34+ CML CFCs. CD34+ cells from 6 CML samples were exposed to increasing doses of BOS. Bar patterns refer to colony-type based on morphology. BFU-E = blast-forming unit-erythroid, CFU-GM = colony-forming unit-granulocyte/ macrophage. Values represent mean ± SEM. I performed all the CFC assays that contributed to this figure.

Figure 3.5.2   CD34+ cells from IM non-responders are sensitive to simultaneous SMO inhibition via PF913 and BCR-ABL1 via BOS. A) Vi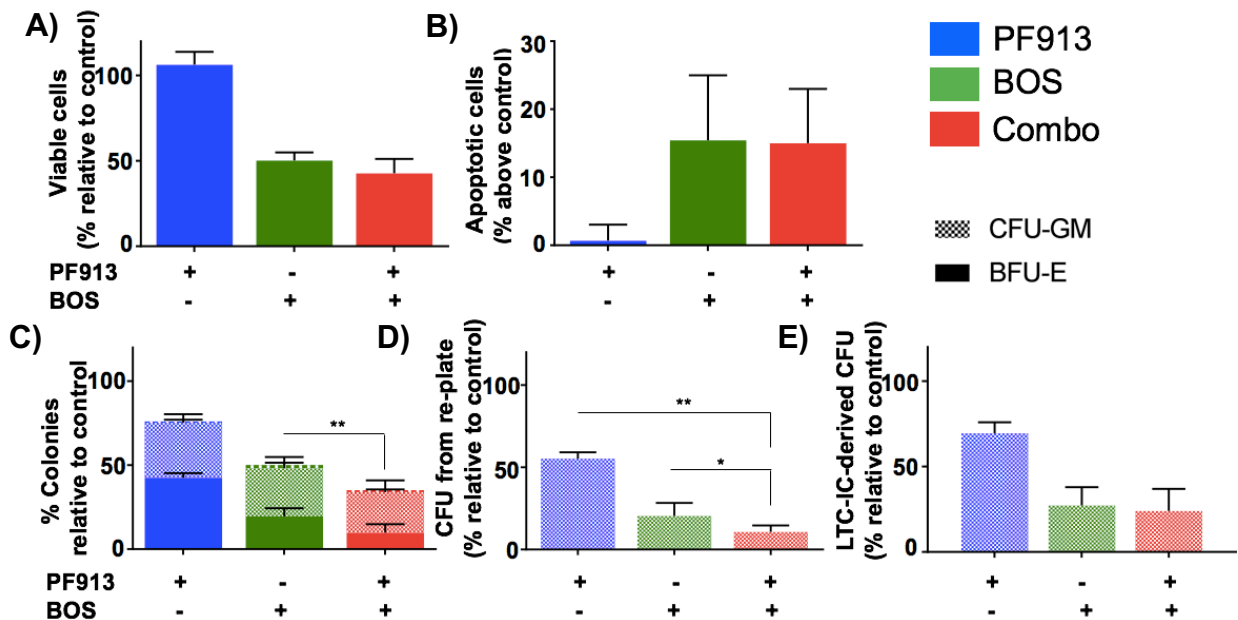ability assay after 72 hours using trypan blue exclusion method. Cells were exposed to 1 μM PF913 ± 0.5 μM BOS (n=3). **B)** Apoptosis assay after 72 hours using Annexin V/PI staining followed by FACS analysis at the

same doses used for the viability experiment (n=3). **C)** CFC assay using 5 μM PF913 and 1 μM BOS (n=3) followed by **D)** Re-plating experiment. **E)** LTC-IC-derived CFC measurements were performed on CD34$^+$ CML cells by exposing cells to 5 μM PF913 and 2 μM BOS for one week followed by half medium changes without drugs for 6 weeks. The cells were cultured on mouse stromal cells for this period. The cells were then harvested and a proportion plated into CFC and colonies enumerated after 2 weeks (n=2). Bar patterns refer to colony-type based on morphology. BFU-E = burst-forming unit-erythroid, CFU-GM = colony-forming unit-granulocyte/ macrophage. All bars represent mean ± SEM. *=p<0.05, **=p<0.01. I performed all the assays that contributed to this figure.

compared with PF913 (55%, p<0.01) and BOS (20%) alone. In the LTC-IC-derived CFC assay

(an *in vitro* stem cell assay), PF913 treatment alone reduced colony-forming unit (CFU) output

by 31% compared with an untreated control (Figure 3.5.2E) and BOS alone reduced CFU

output by 73%, however, the combination was not significantly better than BOS alone (76%

reduction).

3.6   PF913 and BOS are well-tolerated in CD34$^+$ HBM

CFC assays were employed to investigate the toxicity of PF913 and BOS alone,

and in combination in CD34$^+$ HBM samples. Overall, PF913 was very well-tolerated. Indeed,

at doses up to 20 μM, only a 15% reduction in colony-forming ability was observed. For BOS,

colony-forming ability was impaired by 49% at 10 μM (Figure 3.6), suggesting that the doses

used in the CML samples (1-2 μM) would have a minimal detrimental effect on normal cells.

In addition, three different doses of PF913 (1,5,10 μM) were tested in combination with 1 and

2 μM BOS to determine whether the combination used in the CML cells would be toxic to

HBM. At all doses and combinations tested, colony-forming ability was reduced by no more

than 24%.
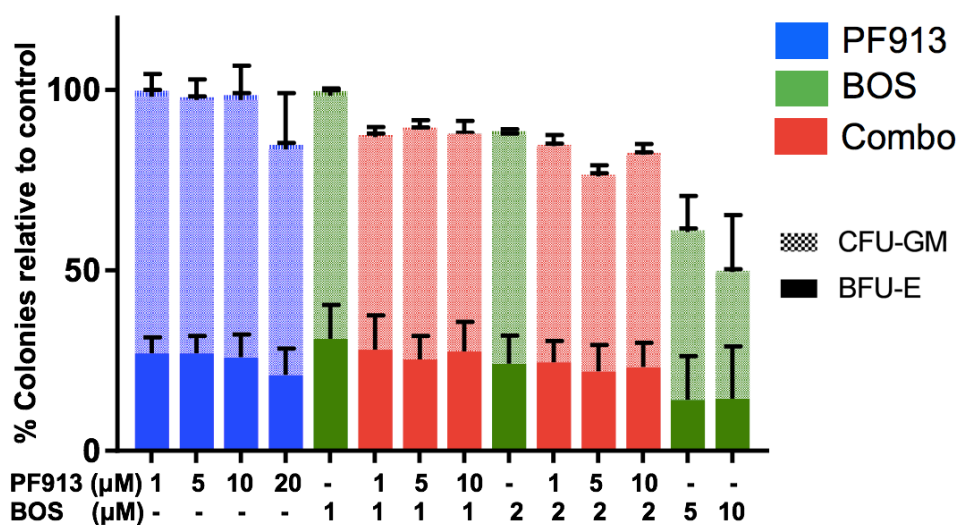
Figure 3.6   PF913 and BOS are well-tolerated by CD34+ HBM cells. CFC assay in 3 HBM samples tested with various doses of PF913 ± BOS. Blue bars correspond to PF913 treatment alone, green bars = BOS treatment alone, red bars = combination. The patterns within the bars correspond to the proportion of colony types based on morphology. BFU-E = burst-forming unit-erythroid, CFU-GM = colony-forming unit-granulocyte/macrophage. Bars represent the mean relative to an untreated control ± SEM. I performed all the CFC assays that contributed to this figure.

3.7   PF913 treatment results in the decreased expression of *GLI2* selectively in CD34+38- CML cells

In order to demonstrate that PF913 could specifically repress the HH pathway via SMO inhibition, I used qRT-PCR to track gene expression changes of downstream HH pathway members *PTCH1, SMO, GLI1* and *GLI2* after treatment. Based on my previous results that the HH pathway, and particularly that *GLI2,* was most highly expressed in the stem-enriched (Lin-CD34+CD38-) subpopulation, I hypothesized that HH pathway inhibition, and consequently *GLI2* suppression, would be strongest in this subpopulation relative to the others. CD34+ cells were cultured overnight (approximately 16 hours) at approximately 5×10^5 cells/mL in serum-free medium with growth factors ± inhibitors. In addition, CD34- cells were retained from the

CD34 enrichment procedure and cultured in the same conditions and used as a control population. Indeed, after overnight exposure to PF913 in combination with BOS, a 53% decrease in expression of *GLI2* was observed in the stem-enriched subpopulation with the combination treatment in patient sample CML IM-NR1. However, no decreases were detected in any of the treatments of the progenitor (Lin$^-$CD34$^+$CD38$^+$) and mature (CD34$^-$) subpopulations in this sample (Figure 3.7A). This finding suggested that the combination was most effective at reducing the expression of *GLI2,* a critical regulator downstream of SMO, selectively in the stem-enriched subpopulation. In contrast, *SMO* expression did not change in any of the CD34-subpopulations in patient sample CML IM-NR1 (Figure 3.7D), as expected, since *SMO* itself is not a downstream target of the *GLI* transcription factors. *PTCH1* and *GLI1* expression also did not change significantly after treatment (data not shown), very likely due to their downregulation at the transcript level in CML cells (Figure 3.1).

A similar, but less striking effect was observed in a second patient sample (CML IM-NR2, Figure 3.7B & E). In the stem-enriched subpopulation, *GLI2* expression was reduced by 25% with the combination treatment, and was relatively unchanged in the progenitor and mature subpopulations (Figure 3.7B). *SMO* (Figure 3.7E)*, GLI1,* and *PTCH1* transcripts remained unchanged across all CD34-subpopulations investigated (data not shown for *GLI1* and *PTCH1*).

In a third patient sample (CML-NR3, Figure 3.7 C & F), *GLI2* expression decreased by 48% in the stem-enriched subpopulation after combination treatment with PF913 and BOS relative to the untreated control, but no changes were observed in the progenitor and mature subpopulations, in agreement with the results demonstrated in the previous patient samples.

However, *SMO* expression also decreased by 48% in the stem-enriched subpopulation in the combination treatment arm relative to an untreated control (Figure 3.7F), which was unexpected. In contrast, there was no change in *SMO* expression in the progenitor and mature subpopulations.

While all patient samples expressed *GLI2* to the greatest extent in the stem-enriched subpopulation, expression in the progenitor subpopulation was less uniform. *GLI2* was similarly expressed in both the stem-enriched and progenitor subpopulation in CML IM-NR1 (Figure 3.7A), but greatly reduced in the progenitor subpopulation relative to the stem-enriched subpopulation in both CML IM-NR2 (Figure 3.7B) and CML IM-NR3 Figure 3.7C), demonstrating the variability of HH pathway activation and expression between different patient samples. *SMO* expression was also variable across different CD34-subpopulations and between different patient samples. Performing this experiment in more patient samples may yield more consistent results.
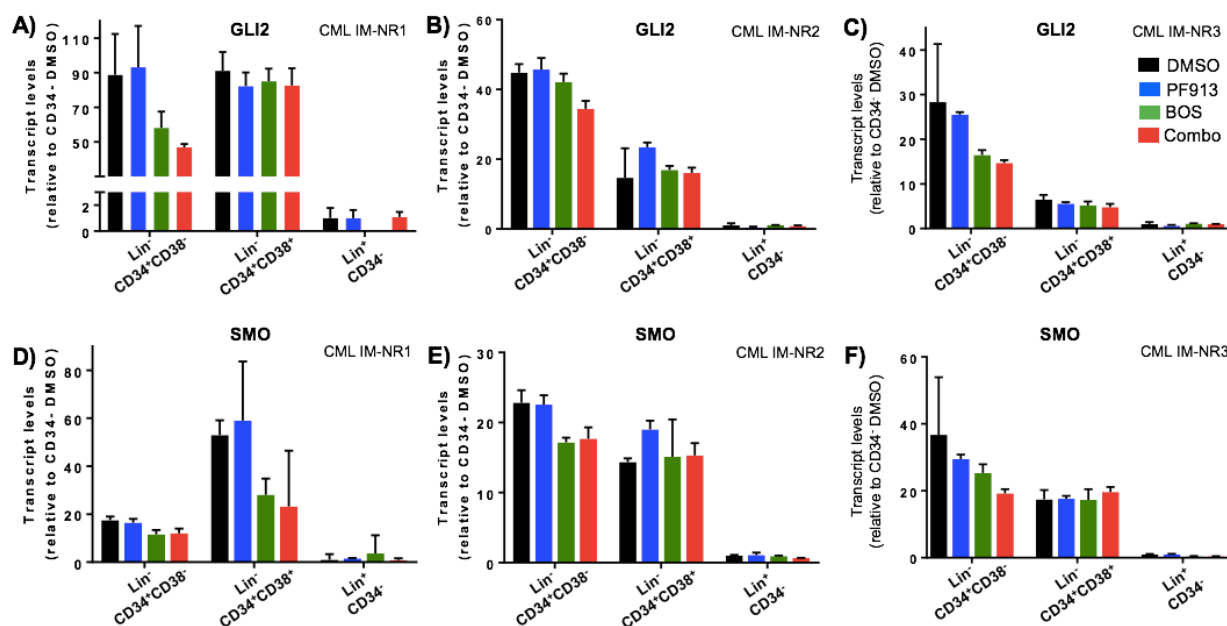
Figure 3.7 **PF913 treatment decreases expression of GLI2 selectively in primary CD34$^+$38$^-$ CML cells. A,B,C)** qRT-PCR analysis of *GLI2* and **D,E,F)** *SMO* expression in subpopulations in three CML IM non-responder patient samples treated with PF913 (5 μM) or BOS (2 μM), alone or in combination for 16 hours in serum-free medium ± inhibitors. Bars represent the mean ± SEM. Cell sorting was assisted by Dr. Wenbo Xu, Flow Core, BC Cancer Agency. I performed all other procedures that contributed to this figure.

41

CHAPTER 4 DISCUSSION

4.1   Discussion

CML treatment has been revolutionized by ABL1 TKIs. However, the disease remains incurable via this approach, in part due to the persistence of drug-insensitive LSCs (Corbin *et al.,* 2010; Chu *et al.,* 2011; Hamilton *et al.,* 2012) which rapidly generate therapy-resistant clones and are responsible for disease relapse in CML patients (Mahon *et al.,* 2011). Recently, it has been proposed that the HH pathway, which is critical during embryonic development, is also important for CML initiation and LSC maintenance (Dierks *et al.,* 2008; Zhao *et al.,* 2009). This has prompted interest in further studies of the HH pathway as a therapeutic target in CML cells. In addition, it was unknown whether the principal HH pathway genes might be differentially expressed in CML cells of IM responders and IM non-responders.

In this study, I investigated expression changes of HH pathway-associated genes in 6 CD34$^+$ CML and 3 HBM control samples revealed by RNA-seq. I discovered that of the 42 HH pathway genes interrogated (Briscoe & Therond, 2013; Kanehisha *et al.,* 2017), 17 were significantly differentially expressed in CML relative to HBM controls (Figure 3.1 and Table 3.1). Interestingly, two of the positive regulators of the HH pathway, *SMO* and *GLI2*, were highly upregulated in CML compared with controls. In addition, when the CML samples were retrospectively characterized as IM responders and IM non-responders, the non-responder samples expressed *GLI2* and *SMO* to a greater extent compared with responders. These results were validated in more patient samples using qRT-PCR (Figure 3.2) and suggest that the HH

pathway is aberrantly expressed in CML cells and may constitute a mechanism by which the LSCs are maintained.

Next, I interrogated the expression of *SMO* and *GLI2* in different CD34-subpopulations in both IM responder and IM non-responder patient samples. *GLI2* was most highly expressed in the stem-enriched, CD34$^+$38$^-$ subpopulation, compared with the progenitor (CD34$^+$38$^+$) and mature (CD34$^-$) subpopulations, whereas *SMO* was more uniformly expressed across the stem-enriched and progenitor subpopulations. When comparing IM responders versus IM non-responders, the IM non-responders expressed both genes to a greater extent compared with the responders, similar to the results obtained in the RNA-seq and qRT-PCR experiments (Figure 3.3). Taken together, I hypothesized that the HH pathway was more critical for CML stem cells in IM non-responders compared with IM responders. Further, I hypothesized that IM non-responders would be more sensitive to HH pathway suppression via the SMO inhibitor PF-04449913 (PF913).

I tested PF913 in CD34$^+$ primary CML patient samples from IM responders and IM non-responders in a variety of assays to determine the effect of the drug on different CML cell populations. Initially, I investigated the effect of SMO inhibition in short-term assays by viability and apoptosis analysis after 72-hour treatment with PF913 (Figure 3.4A & B). At increasing doses of PF913, IM non-responder samples showed a greater reduction in viability and a greater proportion of apoptotic cells relative to the non-responder samples. Next, I tested PF913 on CML progenitor cells by CFC and CFC re-plating assays. The IM non-responder samples were only slightly more impaired in colony-forming ability relative to IM responders in CFC (Figure 3.4C), however, re-plating potential was significantly impaired in IM non-

responders compared with responders (55% vs 107%, p=0.0026, Figure 3.4D), suggesting that more primitive CML cells are more severely impacted by SMO inhibition, particularly in IM non-responders. With this in mind, I focused further studies on IM non-responder patient samples exclusively.

I tested a combination approach of a second generation ABL1 inhibitor bosutinib (BOS) with PF913 in viability, apoptosis, CFC, CFC re-plating and LTC-IC assays. The combination treatment was significantly better at impairing colony-forming ability relative to single treatment with BOS (31% vs 46%, p<0.01, Figure 3.5.2C) and also significantly better at reducing re-plating potential relative to single agent PF913 (11% vs 55%, p<0.01, Figure 3.5.2D), however, the combination was not superior to single agents in LTC-IC assays, which was surprising as HH pathway members *GLI2* and *SMO* were most highly-expressed in the stem-enriched subpopulation, so I hypothesized that pathway inhibition would be most detrimental to this subpopulation (Lin⁻CD34⁺CD38⁻).

A caveat of the LTC-IC assay is that only two patient samples were utilized for this experiment. It is often the case that different patient samples will respond quite differently to drugs across a variety of assays, and these differences are exacerbated in longer term assays that detect more primitive cells. This may be due to the fact that different patient samples harbour differing amounts of residual normal cells (Ph⁻) that can expand in long term assays (Coulombel *et al.,* 1983). Isolating multiple LTC-IC CFC colonies from each treatment arm and performing colony PCR to detect *BCR-ABL1* expression would help to estimate the proportion of normal colonies in the patient sample. As well, performing the assay in more patient samples may yield more generalizable results. Alternatively, it may be that the HH

pathway is critical to a distinct population of leukemic cells that cannot be adequately

evaluated by the LTC-IC assay. For example, it appears as though PF913 alone was most

effective on re-plated cells (45% reduction in CFC output relative to an untreated control),

which represent more primitive progenitor cells, but not quite as primitive as LTC-ICs. To

further tease apart the role of the HH pathway in such a population, cell sorting experiments

followed by qRT-PCR (similar to procedure in Chapter 3.7) could be performed in

intermediate hematopoietic cell types identified phenotypically as common myeloid

progenitors (CMP; $Lin^-CD34^+CD38^+CD123^+CD45RA^-$) granulocyte-macrophage progenitors

(GMP; $Lin^-CD34^+CD38^+CD123^+CD45RA^+$), and megakaryocyte-erythroid progenitors

(MEP; $Lin^-CD34^+CD38^+CD123^-CD45RA^-$; Figure 1.1). Additionally, these cells could be

sorted and then plated into CFC or other assays including viability/apoptosis, to determine the

effects of PF913 and BOS in these more narrowly defined hematopoietic progenitor

populations.

Lastly, I investigated the mechanism by which PF913 suppresses HH pathway activity

by tracking gene expression changes after treatment in different CD34-subpopulations using

qRT-PCR. After overnight exposure to PF913 alone, or in combination with BOS, I sorted the

stem-enriched ($CD34^+38^-$), progenitor ($CD34^+38^+$), and mature ($CD34^-$) subpopulations and

investigated the changes in *SMO, PTCH1, GLI1* and *GLI2* expression after treatment (Figure

3.7). I demonstrated that in three CML IM-NR patient samples, *GLI2* was most highly

expressed in the stem-enriched subpopulation and treatment with a combination of PF913 and

BOS reduced *GLI2* expression the most in the stem-enriched subpopulation. These preliminary

results demonstrate that PF913 and BOS are most effective at reducing *GLI2* in this

subpopulation. In contrast, *SMO, GLI1* and *PTCH1* expression remained mostly unchanged; however, this experiment needs to be repeated in more patient samples to yield more generalizable results due to the variability of expression of *SMO* and *GLI2* between different patient samples.

Notably, a recent study reported by Irvine and colleagues in 2016 used a combination approach with the 2nd generation TKI AMN and SMO inhibitor LDE225 in CP-CML (Irvine *et al.,* 2016). They investigated the expression of HH pathway-associated genes in HSC, CMP, GMP, and MEP subpopulations in HBM and CP-CML samples. Contrary to our results, they did not detect any differences in *GLI2* or *SMO* expression between subpopulations, however, they observed a slight increase in *GLI1* expression (not significant) between 6 CP-CML and 3 HBM samples, whereas we detected a significant decrease with more HBM (n=8) and CP-CML patient samples (n=17; Figure 3.2B). This discrepancy between our results and theirs may be due to the small sample size in the Irvine *et al.* study. Additionally, Irvine *et al.* did not retrospectively characterize their CP-CML patient samples as IM responders or IM non-responders. As I have demonstrated, this distinction greatly influences the observed expression of HH pathway genes. This group also performed CFC re-plating and LTC-IC assays with AMN and LDE225. Similar to my study, from the re-plating assays, they observed significant reductions in CFC output with the combination of drugs compared to cells not exposed to the drugs, albeit at far smaller doses of the SMO inhibitor LDE225 (10 nM). Thus the compound they used may be more potent compared with PF913. They also did not observe a significant reduction in LTC-IC-derived CFC output with the combination relative to the untreated control cells. Again, similar to my results, LDE225 both alone and in combination with AMN,

significantly reduced CFC outputs, but did not eradicate the leukemic cells completely. This lack of effect of the SMO inhibitor alone, in both studies, suggests that the HH pathway may not be activated in a manner that is completely dependent on SMO. Indeed, non-canonical HH signaling, that is, HH signaling that is activated downstream of SMO, has been described in other cancer models (Li *et al.,* 2012; Blotta *et al.,* 2012; Razumilava *et al.,* 2014). Experiments that may tease apart this mechanism in CML are outlined below.

A different study utilizing PF913 in CML was reported by Sadarangani and colleagues (Sadarangani *et al.,* 2015). They performed RNA-seq in 7 CP-CML, 6 BC-CML, 3 normal cord blood, and 3 normal PB progenitor (Lin$^-$CD34$^+$CD38$^+$) samples. Similar to our study, they observed that *GLI2* was significantly differentially expressed between CP-CML and normal controls (p<0.01), but also highly up-regulated in BC-CML samples (approximately 7-fold) compared with CP-CML samples. Deviating from our study, they did not characterize their CP-CML samples as IM responders or IM non-responders. This may have contributed to the observation that very few of the 41 investigated HH pathway-associated genes were significantly differentially expressed.

In co-culture assays with SL/M2 mouse stromal cells genetically engineered to produce human growth factors, they observed that FACS sorted progenitor cells from BC-CML patient samples had impaired survival after 7-day treatment with PF913, however this effect was not observed with normal cord blood cells. This experiment demonstrated that despite being in a supportive niche, BC-CML progenitors were targeted with PF913, likely due to their dependence on *GLI2* expression. I performed similar co-culture assays for 72 hours on M2-10B4 stromal cells that were genetically engineered to secrete human growth factors, and I did

not observe a similar growth disadvantage in CD34$^+$ cells from a CP-CML patient sample. In fact, I observed that the stromal cells were protective and provided a growth advantage, despite SMO inhibition (data not shown). The discrepancy in results may have been due to the fact that different patient samples at different stages of CML were used (BC vs CP) and/or different mouse stromal cell lines were utilized, and have been described to differentially affect CD34$^+$ cells (Koschmieder *et al.,* 2001).

Another aspect of HH signaling that Sadarangani and colleagues explored was the role of GLI2 in CML LSC dormancy (Sadarangani *et al.,* 2015). They observed that CP-CML progenitor cells transduced with GLI2 had a greater proportion of cells in the G0 phase of the cell cycle, compared with cells transduced with the empty vector control or a GLI2 deletion mutant, suggesting that the HH pathway may mediate LSC dormancy and contribute to therapeutic resistance. I did not address this aspect in my study, however, it would be interesting to determine whether there are differences in the G0 fraction in CP-CML samples from IM responders and non-responders (low- and high-expressing *GLI2,* respectively) before and after treatment with PF913. Nevertheless, my study is the first, to my knowledge, that demonstrates that principal HH pathway genes, and most notably *GLI2,* are differentially expressed between IM responders and IM non-responders, and that subsequent HH pathway suppression via PF913 is more detrimental to CD34$^+$ cells from IM non-responders compared with responders in a variety of biological assays.

4.2   Clinical Implications

Clinically, the effectiveness of a combination therapy composed of a TKI and PF913 as a LSC-targeted therapy in CML has yet to be fully determined. In a phase I safety and pharmacokinetics study of PF913 in myeloid malignancies, 5 CML patients were enrolled (2 CP-CML and 3 BC-CML) (Martinelli *et al.,* 2015). The only reported treatment response for this patient group was 1 patient with BC-CML achieved a pCyR. In addition, 60% of all treated patients experienced non-hematological adverse events, the most common being dysgeusia (28%), decreased appetite (19%), and alopecia (15%), and all were grade 1-3 in severity. The authors concluded that a phase II trial was not warranted for CML. However, they recommended that efficacy-focused studies with combination therapies be carried out.

Unfortunately, no studies of that nature have been completed for CML, although encouraging results for AML and myelodysplastic syndrome (MDS) have been reported. A recent phase II study of PF913 in combination with the chemotherapeutic agent Ara-C demonstrated that patients in the combination arm had a longer median overall survival (mOS) compared with patients treated with Ara-C alone (Cortes *et al.,* 2016; NCT01546038). Patients stratified as good/intermediate cytogenetic risk with the combination had a mOS of 12.2 months vs 6.0 months for Ara-C alone, and poor risk patients on the combination had a mOS of 4.4 vs 2.3 months with Ara-C alone. Adverse events associated with PF913 treatment were similar as to what was described in the phase I trial (Martinelli *et al.,* 2015) and overall had an acceptable safety profile.

4.2 Conclusions and Future Directions

In conclusion, I have demonstrated that several key genes involved in regulating the HH pathway, most notably *GLI2,* are deregulated in CML at the transcript level, particularly in CD34$^+$ IM non-responder patient samples and in the most primitive, stem-enriched leukemic cell subpopulation (Lin$^-$CD34$^+$CD38$^-$). Consequently, IM non-responders were more sensitive to SMO inhibition via PF913, suggesting that these patient samples, compared with IM responders, may be activating the HH pathway as a survival mechanism that promotes TKI resistance.

One of the hypotheses of my project was that the HH pathway was critical for the survival of CML stem cells. While I utilized LTC-IC assays to investigate the effects of SMO inhibition on long-term repopulating leukemic cells, I was not looking at a "pure" population of stem cells. The assay enriches for these cells, but overall, I was still analyzing the effects of PF913 on a heterogeneous population. With the advent of multi-colour FACS analysis, it is now possible to significantly enrich for these elusive stem cells using a multitude of surface markers. For example, a population of cells phenotypically defined as CD34$^+$CD38$^-$CD45RA$^-$ CD90$^+$CD49f$^+$ and functionally defined as being able to sustain lymphomyeloid engraftment in NOD-*scid-IL2Rgc$^{-/-}$* (NSG) mice for at least 20 weeks (Notta *et al.,* 2011), contain 10% pure human HSCs. Theoretically, I could try to isolate this population of cells before performing my experiments to ensure that I am investigating a population of cells that might better represent the stem cell compartment and eliminate the need for long-term experiments (such as the LTC-IC assay) because I would start directly with the population of interest. Single cell proliferation experiments, for example, could then be carried out, and the effect of PF913 on

CML LSCs could be better delineated. While theoretically a more efficient and superior approach, it was not possible in this study due to the scarcity of primary patient sample material and the necessity for large numbers of input cells to isolate this rare fraction. In addition, the presence of such cells and confirmation of their inferred stem cell properties or purities in adult HBM has not yet been established.

Another way to investigate the role of the HH pathway in CML would be to investigate the effects of SMO inhibition on LSCs *in vivo.* The severely immunodeficient mouse strain, with genotype $Sirp\alpha^{NOD}$-$Rag1^{-/-}$-$IL2R\gamma c^{-/-}$-$kit^{W41/W41}$, engineered to produce human cytokines IL3, GM-CSF and SCF (SRG-W41-3GS) is an excellent candidate for such a study because it can significantly increase engraftment of human CP-CML patient samples (Nakamichi *et al.,* 2016), which are notoriously difficult to engraft in most other immunodeficient strains. These mice do not develop frank leukemia, however, so a comparison of survival between different treatments cannot not be measured. Instead, SGR-W41-3GS mice could be injected with 2.5×10^6 CD34$^+$ primary CML cells and human cell (CD45$^+$) engraftment monitored long-term (>20 weeks) in PB and BM by FACS. In addition, the amount of human LSCs could be tracked, as well as other human leukemic cell types including myeloid cells (CD33$^+$CD15$^+$), erythroid progenitors (GPA$^+$), etc.

To evaluate drug specificity, SMO knockdown using shRNA or CRISPR/Cas9 should be employed. By genetically knocking down or knocking out *SMO,* respectively, the same assays described above (viability, apoptosis, CFC, LTC-IC, qRT-PCR on HH pathway genes after treatment) could be performed and the results compared with what was obtained using the pharmacological inhibitor PF913. If the results are similar, and importantly, if PF913 is not

more detrimental to cells compared with the knockdown/knockout, then it can be assumed that PF913 specifically inhibits SMO and has minimal off-target effects.

Another question that is raised by this study is the origin of HH pathway activation in CML. Canonical HH signaling begins with the binding of HH ligands to the transmembrane protein *PTCH*. HH ligands can be supplied to the target cell in an autocrine manner or from surrounding stromal cells or other CML cells as a paracrine mechanism. Alternatively, non-canonical HH signaling, that is, activation of *GLI* transcription factors by mechanisms downstream of HH ligand binding, is also possible. Knowing the origin/type of HH signaling in CML is important because it informs which cells will be sensitive to treatment.

Based on our RNA-seq results, *SHH, DHH,* and *IHH* are expressed at very reduced levels in CML cells (all RPKM < 1), making it unlikely that CML cells are supplying themselves or nearby neighbours with HH ligands (Figure 4.1, mechanisms 1&3). Therefore, either supportive stromal cells are supplying HH ligands to CML cells or CML utilizes non-canonical HH signaling. One way to determine whether stromal cells provide HH ligands is to check the expression of SHH, IHH, and DHH at the gene and protein levels using qRT-PCR and Western blotting, respectively, in normal BM stromal cells. To determine whether HH signaling is being activated in a non-canonical fashion, a GLI inhibitor could be utilized.
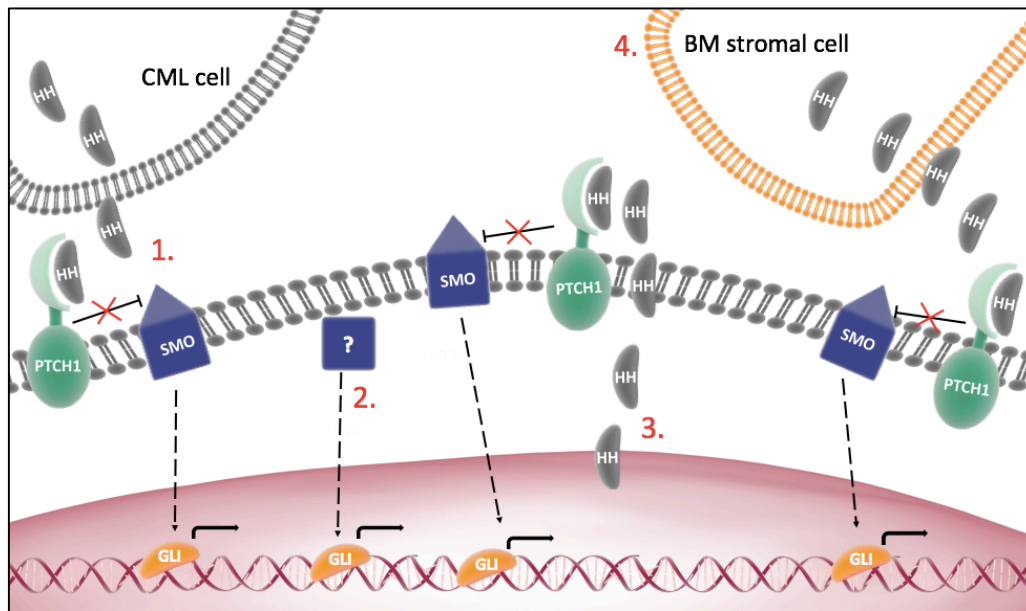
Figure 4.1 **Overview of potential mechanisms of HH signaling in CML. 1)** Paracrine signaling whereby adjacent CML cells produce and secrete HH ligands active on adjacent target cells. **2)** Non-canonical HH signaling. Another protein downstream of SMO activates GLI, driving HH pathway gene expression. **3)** Autocrine signaling. CML cells produce their own supply of HH ligands. **4)** Paracrine signaling from normal stromal cells in the BM microenvironment.

There are currently no GLI inhibitors in clinical trials, however GANT61 is a tool compound and dual GLI1/2 inhibitor that has demonstrated effectiveness in multiple cancer models (Yan *et al.,* 2011; Fu *et al.,* 2013; Srivastava *et al.,* 2014; Wang *et al.,* 2014; Benvenuto *et al.,* 2016). If CML cells are more sensitive to GLI inhibition via GANT61 compared with SMO inhibition via PF913, it may suggest that the HH pathway is being activated in a SMO-independent fashion.

In conclusion, I have demonstrated that several genes in the HH pathway are aberrantly expressed in CP-CML, most notably *SMO* and *GLI2,* particularly in the stem-enriched compartment from IM non-responders. Subsequently, I demonstrated that SMO inhibition by the small molecule PF-04449913 sensitizes CML stem/progenitor cells to TKI treatment with

bosutinib and results in the decreased expression of HH target gene *GLI2,* exclusively in the stem-enriched subpopulation. This study supports the hypothesis that a combination therapy consisting of a HH inhibitor with a TKI may be an effective alternative for TKI resistant patients.

REFERENCES

Agarwal, A., Eide, C.A., Harlow, A., Corbin, A.S., Mauro, M.J., Druker, B.J., Corless, C.L., Heinrich, M.C., Deininger, M.W. 2008. An activating KRAS mutation in imatinib-resistant chronic myeloid leukemia. *Leukemia* **22:** 2269-2272.

Anafi, M., Gazit, A., Gilon, C., Ben-Neriah, Y., Levitzki, A. 1992. Selective interactions of transforming and normal abl proteins with ATP, tyrosine-copolymer substrates, and tyrphostins. *Journal of Biological Chemistry* **267:** 4518-4523.

Baccarani, M., Deininger, M.W., Rosti, G., Hochhaus, A., Soverini, S., Apperley, J.F., Cervantes, F., Clark, R.E., Cortes, J.E., Guilhot, F., Hjorth-Hansen, H., Hughes, T.P., Kantarjian, H.P., Kim, D.W., Larson, R.A., Lipton, J.H., Mahon, F.X., Martinelli, G., Mayer, J., Muller, M.C., Niederwieser, D., Pane, F., Radich, J.P., Rousselot, P., Saglio, G., Sausele, S., Schiffer, C., Silver, R., Simonsson, B., Steegman, J.L., Goldman, J.M., Hehlmann, R. 2013. European LeukemiaNet recommendations for the management of chronic myeloid leukemia: 2013. *Blood* **122:** 872-884.

Baccarani, M., Cortes, J., Pane, F., Niederwieser, D., Saglio, G., Apperley, J., Cervantes, F., Deininger, M.W., Gratwohl, A., Guilhot, F., Hochhaus, A., Horowitz, M., Hughes, T., Kantarjian, H., Larson, R., Radich, J., Simonsson, B., Silver, R.T., Goldman, J., Hehlmann, R. 2009. Chronic myeloid leukemia: An update of concepts and management recommendations of European LeukemiaNet. *Journal of Clinical Oncology* **27:** 6041-6051.

Benjamini, Y. & Yekutieli, D. 2001. The control of the false discovery rate in multiple testing under dependency. *The Annals of Statistics* **29:** 1165-1188.

Bennet, J.H. 1845. Case of hypertrophy of the spleen and liver, which death took place from suppuration of the blood. *Edinburgh Medical and Surgical Journal* **64:** 413-423.

Benvenuto, M., Masuelli, L., De Smaele, E., Fantini, M., Mattera, R., Cucchi, D., Bonanno, E., Di Stefano, E., Frajese, G.V., Orlandi, A., Screpanti, I., Gulino, A., Modesti, A., Bei, R. 2016. In vitro and in vivo inhibition of breast cancer cell growth by targeting the Hedgehog/GLI pathway with SMO (GDC-0449) or GLI (GANT-61) inhibitors. *Oncotarget* **7:** 9250-9270.

Bitgood, M.J. & McMahon, A.P. 1995. Hedgehog and Bmp genes are coexpressed at many diverse sites of cell-cell interaction in the mouse embryo. *Developmental Biology* **172:** 126-138.

Bitgood, M.J., Shen, L., McMahon, A.P. 1996. Sertoli cell signalling by Desert hedgehog regulates the male germline. *Current Biology* **6:** 298-304.

Blotta, S., Jakubikova, J., Calimeri, T., Roccaro, A.M., Amodio, N., Azab, A.K., Foresta, U., Mitsiades, C.S., Rossi, M., Todoerti, K., Molica, S., Morabito, F., Neri, A., Tagliaferri, P., Tassone, P., Anderson, K., Munshi, N.C. 2012. Canonical and noncanonical Hedgehog pathway in the pathogenesis of multiple myeloma. *Blood* **120:** 5002-5013.

Boschelli, D.H., Ye, F., Wang, Y.D., Dutia, M., Johnson, S.L., Wu, B., Miller, K., Powell, D.W., Yaczko, D., Young, M., Tischler, M., Arndt, K., Discafani, C., Etienne, C., Gibbons, J., Grod, J., Lucas, J., Weber, J.M., Boschelli, F. 2001. Optimization of 4-phenylamino-3-quinolinecarbonitriles as potent inhibitors of Src kinase activity. *Journal of Medicinal Chemistry* **44:** 3965-3977.

Briscoe, J. & Therond, P.P. 2013. The mechanisms of Hedgehog signalling and its roles in development and disease. *Nature Reviews Molecular Cell Biology* **14:** 416-429.

Burchert, A., Wang, Y., Cai, D., von Bubnoff, N., Paschka, P., Muller-Bruseelbach, S., Ottman, O.G., Duyster, J., Hochhaus, A., Neubauer, A. 2005. Compensatory PI3-kinase/Akt/mTor activation regulates imatinib resistance development. *Leukemia* **19:** 1774-1782.

Butterfield, Y.S., Kretizman, M., Thiessen, N., Corbett, R.D., Li, Y., Pang, J., Ma, Y.P., Jones, S.J., Birol, I. 2014. JAGuaR: Junction alignments to genome for RNA-seq reads. *PLoS One* **9:** e102398.

Canadian Cancer Society's Advisory Committee on Cancer Statistics. 2016. Canadian Cancer Statistics 2016. Toronto, ON: Canadian Cancer Society. Available at: cancer.ca/Canadian-Cancer-Statistics-2016-EN.pdf (accessed [4 Apr 2017])

Chen, W., Ren, X.R., Nelson, C.D., Barak, L.S., Chen, J.K., Beachy, P.A., de Sauvage, F., Lefkowitz, R.J. 2004. Activity-dependent internalization of smoothened mediated by beta-arrestin 2 and GRK2. *Science* **306:** 2257-2260.

Chu, S., McDonald, T., Lin, A., Chakraborty, S., Huang, Q., Snyder, D.S., Bhatia, R. 2011. Persistence of leukemia stem cells in chronic myelogenous leukemia patients in prolonged remission with imatinib treatment. *Blood* **118:** 5565-5572.

Conan-Doyle, A. 1882. Notes on a case of leucocythaemia. *Lancet* **1882:** 490.

Cooper, O., Hargus, G., Deleidi, M., Blak, A., Osborn, A., Marlow, E., Lee, K., Levy, A., Perez-Torres, E., Yow, A., Isacson, O. 2010. Differentiation of human ES and Parkinson's disease iPS cells into ventral midbrain dopaminergic neurons requires a high activity form of SHH, FGF8a and specific regionalization by retinoic acid. *Molecular and Cellular Neuroscience* **45:** 258-266.

Corbin, A.S., Agarwal, A., Loriaux, M., Cortes, J., Deininger, M.W., Druker, B.J. 2011. Human chronic myeloid leukemia stem cells are insensitive to imatinib despite inhibition of BCR-ABL activity. *The Journal of Clinical Investigation* **121:** 396-409.

Cortes, J.E., Heidel, F.H., Heuser, M., Fiedler, W., Smith, B.D., Robak, T., Fernandez, P.M., Ma, W.W., Shaik, M.N., Zeremski, M., O'Connell, A., Chan, G. 2016. A phase 2 randomized study of low dose Ara-C with or without glasdegib (PF-04449913) in untreated patients with acute myeloid leukemia or high-risk myelodysplastic syndrome. *Blood* **128:** 99.

Cortes, J.E., Kim, D.W., Pinilla-Ibarz, J., le Coutre, P.D., Chuah, C., Nicolini, F.E., Paquette, R., Apperley, J.F., DiPersio, J.F., Khoury, H.J., Rea, D., Talpaz, M., DeAngelo, D.J., Abruzzese, E., Baccarani, M., Mueller, M.C., Gambacorti-Passerini, C., Wong, S., Lustgarten, S., Turner, C.D., Rivera, V.M., Clackson, T., Haluska, F., Kantarjian, H.M., and the PACE Study Group. 2011a. Initial findings from the PACE trial: A pivotal phase 2 study of ponatinib in patients with CML and Ph$^+$ ALL resistant or intolerant to dasatinib or nilotinib, or with the T315I mutation. *Blood* **118:** 109.

Cortes, J.E., Kantarjian, H.M., Brummendorf, T.H., Kim, D.W., Turkina, A.G., Shen, Z.X., Pasquini, R., Khoury, H.J., Arkin, S., Volkert, A., Besson, N., Abbas, R., Wang, J., Leip, E., Gambacorti-Passerini, C. 2011b. Safety and efficacy of bosutinib (SKI-606) in chronic phase Philadelphia chromosome-positive chronic myeloid leukemia patients with resistance or intolerance to imatinib. *Blood* **118:** 4567-4576.

Coulombel, L., Kalousek, D.K., Eaves, C.J., Gupta, C.M., Eaves, A.C. 1983. Long-term marrow culture reveals chromosomally normal hematopoietic progenitor cells in patients with Philadelphia chromosome-positive chronic myelogenous leukemia. *New England Journal of Medicine* **308:** 1493-1498.

Deininger, M., O'Brien, S.G., Guilhot, F., Goldman, J.M., Hochhaus, A., Hughes, T.P., Radich, J.P., Hatfield, A.K., Mone, M., Filian, J., Reynolds, J., Gathmann, I., Larson, R.A., Druker, B.J. 2009. International randomized study of interferon vs STI571 (IRIS) 8-year follow-up: Sustained survival and low risk for progression or events in patients with newly diagnosed chronic myeloid leukemia in chronic phase (CML-CP) treated with imatinib. *Blood* **114:** 1126.

Demurger, F., Ichkou, A., Mougou-Zerelli, S., Le Merrer, M., Goudefroye, G., Delezoide, A.L., … Gonzales, M., Encha-Razavi, F., Odent, S., Vekemans, M., Attie-Bitach, T. 2015. New insights into genotype-phenotype correlation for *GLI3* mutations. *European Journal of Human Genetics* **23:** 92-102.

Dessaud, E., McMahon, A.P., Briscoe, J. 2011. Pattern formation in the vertebrate neural tube: A sonic hedgehog morphogen-regulated transcription network. *Development* **135:** 2489-2503.

Dierks, C., Beigi, R., Guo, G.R., Zirlik, K., Stegert, M.R., Manley, P., Trussell, C., Schmitt-Graeff, A., Landwerlin, K., Veelken, H., Warmuth, M. 2008. Expansion of Bcr-Abl-positive leukemic stem cells is dependent on Hedgehog pathway activation. *Cancer Cell* **14:** 238-249.

Druker, B.J., Talpaz, M., Resta, D.J., Peng, B., Buchdunger, E., Ford, J.M., Lydon, N.B., Kantarjian, H., Capdeville, R., Ohno-Jones, S., Sawyers, C.L. 2001. Efficacy and safety of a specific inhibitor of the BCR-ABL tyrosine kinase in chronic myeloid leukemia.

Druker, B.J., Tamura, S., Buchdunger, E., Ohno, S., Segal, G.M., Fanning, S., Zimmerman, J., Lydon, N.B. 1996. Effects of a selective inhibitor of the Abl tyrosine kinase on the growth of Bcr-Abl positive cells. *Nature Medicine* **2:** 561-566.

Dyer, M.A., Farrington, S.M., Mohn, D., Munday, J.R., Baron, M.H. 2001. Indian hedgehog activates hematopoiesis and vasculogenesis and can respecify prospective neurectodermal cell fate in the mouse embryo. *Development* **128:** 1717-1730.

Echelard, Y., Epstein, D.J., St. Jacques, B., Shen, L., Mohler, J., McMahon, J.A., McMahon, A.P. 1993. Sonic hedgehog, a member of a family of putative signalling molecules, is implicated in the regulation of CNS polarity. *Cell* **75:** 1417-1430.

Ericson, J., Briscoe, J., Rashbass, P., van Heyningen, V., Jessell, T.M. 1997. Graded sonic hedgehog signaling and the specification of cell fate in the ventral neural tube. *Cold Spring Harbour Symposia on Quantitative Biology* **62:** 451-466.

Fefer, A., Cheever, M.A., Thomas, E.D., Boyd, C., Ramberg, R., Glucksberg, H., Buckner, C.D., Storb, R. 1979. Disappearance of pH[1]-positive cells in four patients with chronic granulocytic leukemia after chemotherapy, irradiation and marrow transplantation from an identical twin. *New England Journal of Medicine* **300:** 333-337.

Fu, J., Rodova, M., Roy, S.K., Sharma, J., Singh, K.P., Srivastava, R.K., Shankar, S. 2013. GANT-61 inhibits pancreatic stem cell growth in vitro and in NOD/SCID/IL2R gamma null mice xenograft. *Cancer Letters* **330:** 22-32.

Gesbert, F., Seller, W.E., Signoretti, S., Loda, M., Griffin, J.D. 2000. BCR/ABL regulates expression of the cyclin-dependent kinase inhibitor p27[Kip1] through the phosphatidylinositol 3-kinase/AKT pathway. *The Journal of Biological Chemistry* **275:** 39223-39230.

Giles, F.J., O'Dwyer, M., Swords, R. 2009. Class effects of tyrosine kinase inhibitors in the treatment of chronic myeloid leukemia. *Leukemia* **23:** 1698-1707.

Gioia, R., Leroy, C., Drullion, C., Lagarde, V., Etienne, G., Dulucq, S., Lippert, E., Roche, S., Mahon, F.X., Pasquet, J.M. 2011. Quantitative phosphoproteomics revealed interplay between Syk and Lyn in the resistance to nilotinib in chronic myeloid leukemia cells. *Blood* **118:** 2211-2221.

Goetz, S.C. & Anderson, K.V. 2010. The primary cilium: A signalling centre during vertebrate development. *Nature Reviews Genetics* **11:** 331-334.

Golas, J.M., Arndt, K., Etienne, C., Lucas, J., Nardin, D., Gibbons, J., Frost, P., Ye, F., Boschelli, D.H., Boschelli, F. 2003. SKI-606, a 4-anilino-3-quinolinecarbonitrile dual inhibitor of Scr and Abl kinases, is a potent antiproliferative agent against chronic myelogenous leukemia cells in culture and causes regression of K562 xenografts in nude mice. *Cancer Research* **63:** 375-381.

Gorlin, R.J. 2004. Nevoid basal cell carcinoma (Gorlin) syndrome. *Genetics in Medicine* **6:** 530-539.

Gorre, M.E., Mohammed, M., Ellwood, K., Hsu, N., Paquette, R., Rao, P.N., Sawyers, C.L. 2001. Clinical resistance to STI-571 cancer therapy caused by BCR-ABL gene mutation or amplification. *Science* **293:** 876-880.

Grossman, V., Kohlmann, A., Zenger, M., Schindela, S., Eder, C., Weissmann, S., Schnittger, S., Kern, W., Muller, M.C., Hochhaus, A., Haferlach, T., Haferlach, C. 2011. A deep-sequencing study of chronic myeloid leukemia patients in blast crisis (BC-CML) detects mutations in 76.9% of cases. *Leukemia* **25:** 557-560.

Hamilton, A., Helgason, G.V., Schemionek, M., Zhang, B., Myssina, S., Allan, E.K., Nicolini, F.E., Muller-Tidow, C., Bhatia, R., Brunton, V.G., Koschmieder, S., Holyoake, T.L. 2012. Chronic myeloid leukemia stem cells are not dependent of Bcr-Abl kinase activity for their survival. *Blood* **119:** 1501-1510.

Hammerschmidt, M., Brook, A., McMahon, A.P. 1997. The world according to hedgehog. *Trends in Genetics* **13:** 14-21.

Haut, A., Abbott, W.S., Wintrobe, M.M., Cartwright, G.E. 1961. Busulfan in the treatment of chronic myelocytic leukemia: The effect of long term intermittent therapy. *Blood* **17:** 1-19.

Hehlmann, R., Heimpel, H., Hasford, J., Kolb, H.J., Pralle, H., Hossfeld, D.K., Queisser, W., Loffler, H., Hochhaus, A., Heinze, B, *et al.* 1994. Randomized comparison of interferon-alpha with busulfan and hydroxyurea in chronic myelogenous leukemia. The German CML Study Group. *Blood* **84:** 4064-4077.

Hehlmann, R., Heimpel, H., Hasford, J., Kolb, H.J., Pralle, H., Hossfeld, D.K., Queisser, W., Loffler, H., Heinze, B., Georgii, A. 1993. Randomized comparison of busulfan and hydroxyurea in chronic myelogenous leukemia: Prolongation of survival by hydroxyurea. The German CML Study Group. *Blood* **82:** 398-407.

Hogge, D.E., Lansdorp, P.M., Reid, D., Gerhard, B., Eaves, C.J. 1996. Enhanced detection, maintenance, and differentiation of primitive human hematopoietic cells in cultures containing murine fibroblasts engineered to produce human steel factor, interleukin-3, and granulocyte colony-stimulating factor. *Blood* **88:** 3765-3773.

Holyoake, T.L., Jiang, X., Eaves, C., Eaves, A. 1999. Isolation of a highly quiescent subpopulation of primitive leukemic cells in chronic myeloid leukemia. *Blood* **94:** 2056-2064.

Illmer, T., Schaich, M., Platzbecker, U., Freiberg-Richter, J., Oelschlagel, U., von Bonin, M., Pursche, S., Bergemann, T., Ehninger, G., Schleyer, E. 2004. P-glycoprotein-mediated drug efflux is a resistance mechanism of chronic myelogenous leukemia cells to treatment with imatinib mesylate. *Leukemia* **18:** 401-408.

Irvine, D.A., Zhang, B., Kinstrie, R., Tarafdar, A., Morrison, H., Campbell, V.L., Moka, H.A., Ho, Y., Nixon, C., Manley, P.W., Wheadon, H., Goodlad, J.R., Holyoake, T.L., Bhatia, R., Copland, M. 2016. Deregulated hedgehog pathway signaling is inhibited by the smoothened antagonist LDE225 (Sonidegib) in chronic phase chronic myeloid leukemia. *Scientific Reports* **6:** 25476.

Jagani, Z., Song, K., Kutok, J.L., Dewar, M.R., Melet, A., Santos, T., Grassian, A., Ghaffari, S., Wu, C., Ren, R., Rodin, H.Y., Miller, K., Khosravi-Far, R. 2008. Proteasome inhibition causes regression of leukemia and abrogates BCR-ABL-induced evasion of apoptosis in part through regulation of forkhead tumor suppressors. *Biochimica et Biophysica Acta (BBA)-Reviews on Cancer* **1785:** 63-84.

Jiang, X., Saw, K.M., Eaves, A., Eaves, C. 2007a. Instability of BCR-ABL gene in primary and cultured chronic myeloid leukemia stem cells. *Journal of the National Cancer Institute.* **99:** 680-693.

Jiang, X., Zhao, Y., Smith, C., Gasparetto, M., Turhan, A., Eaves, A., Eaves, C. 2007b. Chronic myeloid leukemia stem cells possess multiple unique features of resistance to BCR-ABL targeted therapies. *Leukemia* **21:** 926-935.

Kanehisha, M., Furumichi, M., Tanabe, M., Sato, Y., Morishima, K. 2017. KEGG: New perspectives on genomes, pathways, diseases and drugs. *Nucleic Acids Research* **45:** D353-D361.

Kang, S., Graham, J.M. Jr., Olney, A.H., Biesecker, L.G. 1997. GLI3 frameshift mutations cause autosomal dominant Pallister-Hall syndrome. *Nature Genetics* **15:** 266-268.

Kantarjian, H. 2016. The arrival of generic imatinib into the U.S. market: An educational event. *The ASCO Post* **7:** 110-111.

Keller-von Amsberg, G. & Koschmieder, S. 2013. Profile of bosutinib and its clinical potential in the treatment of chronic myeloid leukemia. *OncoTargets and Therapy* **6:** 99-106.

Kennedy, B.J. & Yarbro, J.W. 1966. Metabolic and therapeutic effects of hydroxyurea in chronic myeloid leukemia. *Journal of the American Medical Association* **195:** 1038-1043.

Kenney, A.M., Cole, M.D., Rowitch, D.H. 2003. Nmyc upregulation by sonic hedgehog signaling promotes proliferation in developing cerebellar granule neuron precursors. *Development* **130:** 15-28.

Kenney, A.M. & Rowitch, D.H. 2000. Sonic hedgehog promotes G_1 cyclin expression and sustained cell cycle progression in mammalian neuronal precursors. *Molecular and Cellular Biology* **20:** 9055-9067.

Kim, T.H., Tyndel, M.S., Kim, H.J., Ahn, J.S., Choi, S.H., Park, H.J., Kim, Y.K., Kim, S.Y., Lipton, J.H., Zhang, Z., Kim, D.D.H. 2017. Spectrum of somatic mutation dynamics in chronic myeloid leukemia following tyrosine kinase inhibitor therapy

Konig, K., Holyoake, T.L., Bhatia, R. 2008. Effective and selective inhibition of chronic myeloid leukemia primitive hematopoietic progenitors by the dual Src/Abl kinase inhibitor SKI-606. *Blood* **111:** 2329-2338.

Koptyra, M., Falinski, R., Nowicki, M.O., Stoklosa, T., Majsterek, I., Nieborowska-Skorsa, M., Blasiak, J., Skorski, T. 2006. BCR/ABL kinase induces self-mutagenesis via reactive oxygen species to encode imatinib resistance. *Blood* **108:** 319-327.

Koschmieder, S., Bug, G., Schroeder, B., Rossmanith, T., Hofmann, W.K., Kalina, U., Hoelzer, D., Ottman, O.G. 2001. Murine M2-10B4 and SL/SL cell lines differentially affect the balance between CD34$^+$ cell expansion and maturation. *International Journal of Hematology* **73:** 71-77.

Kovacs, J.J., Whalen, E.J., Liu, R., Xiao, K., Kim, J., Chen, M., Wang, J., Chen, W., Lefkowitz, R.J. 2008. Beta-arrestin-mediated localization of smoothened to the primary cilium. *Science* **320:** 1777-1781.

Kruger, G., Gotz, J., Kvist, U., Dunker, H., Erfurth, F., Pelz, L., Zech, L. 1989. Greig syndrome in a large kindred due to reciprocal chromosome translocation t(6;7)(q27;p13). *American Journal of Medical Genetics* **32:** 411-416.

Kubo, M., Nakamura, M., Tasaki, A., Yamanaka, N., Nakashima, H., Nomura, M., Kuroki, S., Katano, M. 2004. Hedgehog signaling pathway is a new therapeutic target for patients with breast cancer. *Cancer Research* **64:** 6071-6074.

le Coutre, P., Tassi, E., Varella-Garcia, M., Barni, R., Mologni, L., Cabrita, G., Marchesi, E., Supino, S., Gambacorti-Passerini, C. 2000. Induction of resistance to the Abelson inhibitor STI571 in human leukemic cells through gene amplification. *Blood* **95:** 1758-1766.

Li, H., Handsaker, B., Wysoler, A., Fennell, T., Ruan, J., Homer, N., Marth, G., Abecasis, G., Durbin, R., 1000 Genome Project Data Processing Subgroup. 2009. The sequence alignment/map format and SAMtools. *Bioinformatics* **25:** 2078-2079.

Li, X., Ma, Q., Xu, Q., Liu, H., Lei, J., Duan, W, Bhat, K., Wang, F., Wu, E., Wang, Z. 2012. SDF-1/CXCR4 signaling induces pancreatic cancer cell invasion and epithelial-mesenchymal transition in vitro through non-canonical activation of Hedgehog pathway. *Cancer Letters* **322:** 169-176.

Lupo, G., Harris, W.A., Lewis, K.E. 2006. Mechanisms of ventral patterning in the vertebrate nervous system. *Nature Reviews Neuroscience* **7:** 103-114.

Ma, X., Chen, K., Huang, S., Zhang, X., Adegboyega, P.A., Evers, B.M., Zhang, H., Xie, J. 2005. Frequent activation of the hedgehog pathway in advanced gastric adenocarcinomas. *Carcinogenesis* **26:** 1698-1705.

Mahon, F.X., Rea, D., Guilhot, J., Guilhot, F., Huguet, F., Nicolini, F.E., Legros, L., Charbonnier, A., Guerci, A., Varet, B.R., Etienne, G., Reiffers, J., Rousselot, P. 2011. Discontinuation of imatinib in patients with chronic myeloid leukemia who have maintained complete molecular responder: Update results of the STIM study. *Blood* **118:** 603.

Mahon, F.X., Rea, D., Guilhot, J., Guilhot, F., Huguet, F., Nicolini, F., Legros, L. 2010. Discontinuation of imatinib in patients with chronic myeloid leukaemia who have maintained complete molecular remission for at least 2 years: The prospective, multicentre Stop Imatinib (STIM) trial. *The Lancet Oncology* **11:** 1029-1035.

Martinelli, G., Oehler, V.G., Papayannidis, C., Courtney, R., Shaik, M.N., Zhang, X., O'Connell, A., McLachlan, K.R., Zheng, X., Radich, J., Baccarani, M., Kantarjian, H.M., Levin, W.J., Cortes, J.E., Jamieson, C. 2015. Treatment with PF-04449913, an oral smoothened antagonist, in patients with myeloid malignancies: a phase 1 safety and pharmacokinetics study. *Lancet Haematology* **2:** e339-e346.

Massimino, M., Consoli, M.L., Mesuraca, M., Stagno, F., Tirro, E., Stella, S., Pennisi, M.S., Romano, C., Buffa, P., Bond, H.M., Morrone, G., Sciacca, L., Di Raimondo, F., Manzella, L., Vigneri, P. 2014. IRF5 is a target of BCR-ABL kinase activity and reduces CML cell proliferation. *Carcinogenesis* **35:** 1132-1143.

McGlave, P.B., De Fabritiis, P., Deisseroth, A., Goldman, J., Barnett, M., Reiffers, J., Simonsson, B., Carella, A., Aeppli, D. 1994. Autologous transplants for chronic myelogenous leukaemia: Results from eight transplant groups. *Lancet* **343:** 1486-1488.

Ming, J.E., Kaupas, M.E., Roessler, E., Brunner, H.G., Golabi, M., Tekin, M., Stratton, R.F., Sujanksy, E., Bale, S.J., Muenke, M. 2002. Mutations in PATCHED-1, the receptor for SONIC HEDGEHOG, are associated with holoprosencephaly. *Human Genetics* **110:** 297-301.

Nakamichi, N., Hammond, C.A., Miller, P.H., Rothe, K., Beer, P.A., Jiang, X., Deininger, M.W., Eaves, C.J. 2016. Enhanced and accelerated repopulation of mutant *c-Kit* immunodeficient mice by transplants of primary chronic and acute myeloid leukemic human cells. *Blood* **128:** 4537.

Niewiadomski, P., Kong, J.H., Ahrends, R., Ma, Y., Humke, E.W., Khan, S., Teruel, M.N., Novitch, B.G., Rohatgi, R. 2014. Gli protein activity is controlled by multisite phosphorylation in vertebrate Hedgehog signalling. *Cell Reports* **6:** 168-181.

Notta, F., Doulatov, S., Laurenti, E., Poeppl, A., Jurisica, I., Dick, J.E. 2011. Isolation of single human hematopoietic stem cells capable of long-term multilineage engraftment. *Science* **333:** 218-221.

Nowell, P.C. & Hungerford, D.A. 1960. A minute chromosome in human chronic granulocytic leukemia. *Science* **142:** 1497.

Nusslein-Volhard, C. & Wieschaus, E. 1980. Mutations affecting segment number and polarity in *Drosophila. Nature* **287**: 795-801.

O'Brien, S., Guilhot, F., Larson, R.A., Gathmann, I., Baccarani, M., Cervantes, F., Cornelissen, J.J., Fischer, T., Hochhaus, A., Hughes, T., Lechner, K., *et al.* and the IRIS Investigators. 2003. Imatinib compared with interferon and low-dose cytarabine for newly diagnosed chronic-phase chronic myeloid leukemia. *New England Journal of Medicine* **348:** 994-1004.

Oro, A.E., Higgins, K.M., Hu, Z., Bonifas, J.M., Epstein, E.H. Jr., Scott, M.P. 1997. Basal cell carcinomas in mice overexpressing sonic hedgehog. *Science* **276:** 817-821.

Petrova, R. & Joyner, A.L. 2014. Roles for Hedgehog signaling in adult organ homeostasis and repair. *Development* **141:** 3445-3457.

Puttini, M., Coluccia, A.M.L., Boschelli, F., Cleris, L., Marchesi, E., Donella-Deana, A., Ahmed, S., Redaelli, S., Piazza, R., Magistroni, V., Andreoni, F., Scapozza, L., Formelli, F., Gambacorti-Passerini, C. 2006. In vitro and in vivo activity of SKI-606, a novel Src-Abl inhibitor against imatinib-resistant Bcr-Abl^{+} neoplastic cells. *Cancer Research* **66:** 11314-11322.

Quintas-Cardama, A. & Cortes, J.E. 2006. Chronic myeloid leukemia: Diagnosis and treatment. *Mayo Clinic Proceedings* **81:** 973-988.

Radhakrishna, U., Wild, A., Grzeschik, K.H., Antonarakis, S.E. 1997. Mutation in *GLI3* in postaxial polydactyly type A. *Nature Genetics* **17:** 269-271.

Razumilava, N., Gradilone, S.A., Smoot, R.L., Mertens, J.C., Bronk, S.F., Sirica, A.E., Gores, G.J. 2014. Non-canonical Hedgehog signalling contributes to chemotaxis in cholangiocarcinoma. *Journal of Hepatology* **60:** 599-605.

Redaelli, S., Piazza, R., Rostagno, R., Magistroni, V., Perini, P., Marega, M., Gambacorti-Passerini, C., Boschelli, F. 2009. Activity of bosutinib, dasatinib, and nilotinib against 18 imatinib-resistant BCR/ABL mutants. *Journal of Clinical Oncology* **27:** 469-471.

Riddle, R.D., Johnson, R.L., Laufer, E., Tabin, C. 1993. Sonic hedgehog mediates the polarising activity of the ZPA. *Cell* **75:** 1401-1416.

Roessler, E., Du, Y.Z., Mullor, J.L., Casas, E., Allen, W.P., Gillessen-Kaesbach, G., Roeder, E.R., Ming, J.E., Altaba, A.R., Muenke, M. 2003. Loss-of-function mutations in the human *GLI2* gene are associated with pituitary anomalies and holoprosencephaly-like features. *Proceesings of the National Academy of Sciences USA* **100:** 13424-13429.

Roessler, E., Belloni, E., Gaudenz, K., Jay, P., Berta, P., Scherer, S.W., Tsui, L.C., Muenke, M. 1996. Mutations in the human Sonic Hedgehog gene cause holoprosencephaly. *Nature Genetics* **14:** 357-360.

Rothe, K., Lin, H., Lin, K.B.L., Leung, A., Wang, H.M., Malekesmaeili, M., Brinkman, R.R., Forrest, D.L., Gorski, S.M., Jiang, X. 2014. The core autophagy protein ATG4B is a potential biomarker and therapeutic target in CML stem/progenitor cells. *Blood* **123:** 3622-3634.

Rowley, J.D. 1973. A new consistent chromosomal abnormality of chronic myelogenous leukaemia identified by quinacrine fluorescence and Giemsa staining. *Nature* **243:** 290-293.

Ruat, M., Hoch, L., Faure, H., Rognan, D. 2014. Targeting of Smoothened for therapeutic gain. *Trends in Pharmacological Sciences* **35:** 237-246.

Sadarangani, A., Pineda, G., Lennon, K.M., Chun, H.J., Shih, A., Schairer, A.E., Court, A.C., Goff, D.J., Prashad, S.L., Geron, I., Wall, R., McPherson, J.D., Moore, R.A., Pu, M., Bao, L., Jackson-Fisher, A., Munchhof, M. VanArsdale, T., Reya, T., Morris, S.R., Minden, M.D., Messer, K., Mikkola, H.K.A., Marra, M.A., Hudson, T.J., Jamieson, C.H.M. 2015. GLI2 inhibition abrogates human leukemia stem cell dormancy.

Saldana, J.I., Solkani, A., Lau, C.I., Sahni, H., Ross, S., Furmanski, A.L., Ono, M., Hollander, G., Crompton, T. 2016. Sonic hedgehog regulates thymic epithelial cell differentiation. *Journal of Autoimmunity* **68:** 86-97.

Sawyers, C.L., Hochhaus, A., Feldman, E., Goldman, J.M., Miller, C.B., Ottman, O.G., Schiffer, C.A., Talpaz, M., Guilhot, F., Deininger, M., Fischer, T. O'Brien, S.G., Stone, R.M., *et al.* 2002. Imatinib induces hematologic and cytogenetic responses in patients with chronic myelogenous leukemia in myeloid blast crisis: Results of a phase II study. *Blood* **99:** 3530-3539.

Speck, B., Bortin, M.M., Champlin, R., Goldman, J.M., Herzig, R.H., McGlave, P.B., Messner, H.A., Weiner, R.S., Rimm, A.A. 1984. Allogeneic bone marrow transplantation for chronic myelogenous leukaemia. *Lancet* **323:** 665-668.

Srivastava, R.K., Kaylani, S.Z., Edrees, N., Li, C., Talwelkar, S.S., Xu, J., Palle, K., Pressey, J.G., Athar, M. 2014. GLI inhibitor GANT-61 diminishes embryonal and alveolar rhabdomyosarcoma growth by inhibiting Shh/AKT-mTOR axis. *Oncotarget* **5:** 12151-12165.

St. Jacques, B., Hammerschmidt, M., McMahon, A.P. 1999. Indian hedgehog signaling regulates proliferation and differentiation of chrondrocytes and is essential for bone formation. *Genes & Development* **13:** 2072-2086.

Steelman, L.S., Pohnert, S.C., Shelton, J.G., Franklin, R.A., Bertrand, F.E., McCubrey, J.A. 2004. JAK/STAT, Raf/MEK/ERK, PI3K/Akt and BCR-ABL in cell cycle progression and leukemogenesis. *Leukemia* **18:** 189-218.

Taipale, J., Cooper, M.K., Maiti, T., Beachy, P.A. 2002. Patched acts catalytically to suppress the activity of Smoothened. *Nature* **418:** 892-896.

Talpaz, M., Silver, R.T., Druker, B.J., Goldman, J.M., Gambacorti-Passerini, C., Guilhot, F., Schiffer, C.A., Fischer, T., Deininger, M., Lennard, A.L., Hochhaus, A., Ottman, O.G., *et al.* 2002. Imatinid induces durable hematologic and cytogenetic responses in patients with accelerated phase chronic myeloid leukemia: Results of a phase 2 study. *Blood* **99:** 1928-1937.

Talpaz, M., Kantarjian, H.M., McCredie, K., Trujillo, J.M., Keating, M.J., Gutterman, J.U. 1986. Hematologic remission and cytogenetic improvement by recombinant human interferon alpha A in chronic myelogenous leukemia. *New England Journal of Medicine* **314:** 1065-1069.

Thayer, S.P., di Magliano, M.P., Heiser, P.W., Nielsen, C.M., Roberts, D.J., Lauwers, G.Y., Qi, Y.P., Gysin, S., Fernandez-del Castillo, C., Yajnik, V., Antoniu, B., McMahon, M., Warshaw, A.L., Hebrok, M. 2003. Hedgehog is an early and late mediator of pancreatic cancer tumorigenesis. *Nature* **425:** 851-856.

Tough, I.M., Court Brown, W.M., Baikie, A.G., Buckton, K.E., Harnden, D.G., Jacobs, P.A., King, M.J., McBride, J.A. 1961. Cytogenetic studies in chronic myeloid leukaemia and acute leukaemic associated with mongolism. *Lancet* **7174:** 411-417.

Tseng, T.T., Gratwick, K.S., Kollman, J., Park, D., Nies, D.H., Goffeau, A., Saier, M.H. 1999. The RNS permease superfamily: An ancient, ubiquitous and diverse family that includes human disease and development proteins. *Journal of Molecular Microbiology and Biotechnology* **1:** 107-125.

Tsukui, T., Capdevila, K., Tamura, P., Ruiz-Lozano, P., Rodriguez-Esteban, C., Yonei-Tamura, S., Magallon, J., Chandraratna, R.A., Chien, K., Blumberg, B., Evans, R.M., Belmonte, J.C. 1999. Multiple left-right asymmetry defects in *Shh(-/-)* mutant mice unveil a convergence of the shh and retinoic acid pathways in the control of Lefty-1. *Proceedings of the National Academy of Sciences USA* **96:** 11376-11381.

Tukachinsky, H., Petrov, K., Watanabe, M., Salic, A. 2016. Mechanism of inhibition of the tumor suppressor Patched by Sonic Hedgehog. *Proceedings of the National Academy of Sciences* **113:** E5866-E5875

Vianello, F., Villanova, F., Tisato, V., Lymperi, S., Ho, K.K., Gomes, A.R., Marin, D., Bonnet, D., Apperley, J., Lam, E.W.F., Dazzi, F. 2010. Bone marrow mesenchymal stromal cells non-selectively protect chronic myeloid leukemia cells from imatinib-induced apoptosis via the CXCR4/CXCL12 axis. *Haematologica* **95:** 1081-1089.

Wang, J., Gu, S., Huang, J., Chen, S., Zhang, Z., Xu, M. 2014. Inhibition of autophagy potentiates the efficacy of Gli inhibitor GANT-61 in MYCN-amplified neuroblastoma cells. *BMC Cancer* **14:** 768.

Wang, L., Giannoudis, A., Lane, S., Williamson, P., Pirmohamed, M., Clark, R.E. 2008. Expression of the uptake drug transporter hOCT1 is an important clinical determinant of the response to imatinib in chronic myeloid leukemia. *Clinical Pharmacology and Therapeutics* **83:** 258-264.

Wang, Y., Cai, D., Brendel, C., Barett, C., Erben, P., Manley, P.W., Hochhaus, A., Neubauer, A., Burchert, A. 2007. Adaptive secretion of granulocyte-macrophage colony-stimulating factor (GM-CSF) mediates imatinib and nilotinib resistance in BCR/ABL+ progenitors via JAK-2/STAT-5 pathway activation. *Blood* **109:** 2147-2155.

Watkins, D.N., Berman, D.M., Burkholder, S.G., Wang, B., Beachy, P.A., Baylin, S.B. 2003. Hedgehog signalling within airway epithelial progenitors and in small-cell lung cancer. *Nature* **422:** 313-317.

Wei, G., Rafiyath, S., Liu, D. 2010. First-line treatment for chronic myeloid leukemia: Dasatinib, nilotinib, or imatinib. *Journal of Hematology & Oncology* **3:** 47-57.

Weissman, I.L. & Shizuru, J.A. 2008. The origins of the identification and isolation of hematopoietic stem cells, and their capability to induce donor-specific transplantation tolerance and treat autoimmune diseases. *Blood* **112:** 3543-3553.

Wellbrock, J., Latuske, E., Kohler, J., Wagner, K., Stamm, H., Vettorazzi, E., Vohwinkel, G., Klokow, M., Uibeleisen, R., Ehm, P., Riecken, K., Loges, S., Thol, F., Schubert, C., Amling, M., Jucker, M., Bokemeyer, C., Heuser, M., Krauter, J., Fiedler, W. 2015. Expression of hedgehog pathway mediator GLI represents a negative prognostic marker in human acute myeloid leukemia and its inhibition exerts antileukemic effects. *Clinical Cancer Research* **21:** 2388-2398.

Wen, X., Lai, C.K., Evangelista, M., Hongo, J.A., de Sauvage, F.J., Scales, S.J. 2010. Kinetics of hedgehog-dependent full-length Gli3 accumulation in primary cilia and subsequent degradation. *Molecular Cell Biology* **30:** 1910-1922.

Wild, A., Kalff-Suske, M., Vortkamp, A., Bornholdt, D., Konig, R., Grzeschik, K.H. 1997. Point mutations in human GLI3 cause Greig syndrome. *Human Molecular Genetics* **6:** 1979-1984.

Wu, C., Shimo, T., Liu, M., Pacifici, M., Koyama, E. 2003. Sonic hedgehog functions as a mitogen during bell stage of odontogenesis. *Connective Tissue Research* **44:** 92-96.

Yan, M., Wang, L., Zuo, H., Zhang, Z., Chen, W., Mao, L., Zhang, P. 2011. HH/GLI signalling as a new therapeutic target for patients with oral squamous cell carcinoma. *Oral Oncology* **47:** 504-509.

Zhao, C., Chen, A., Jamieson, C.H., Fereshteh, M., Abrahamsson, A., Blum, J., Kwon, H.Y., Kim, J., Chute, J.P., Rizzieri, D., Munchhof, M., VanArsdale, T., Beachy, P.A., Reya, T. 2009. Hedgehog signalling is essential for maintenance of cancer stem cells in myeloid leukemia. *Nature* **458:** 776-779.